(12) INTERNATIONAL APPLICATION PUBLISHED UNDER THE PATENT COOPERATION TREATY (PCT)

(19) World Intellectual Property Organization
International Bureau

(43) International Publication Date
16 March 2017 (16.03.2017)

WIPO | PCT

(10) International Publication Number
WO 2017/044768 A1

(51) International Patent Classification:
C12N 15/113 (2010.01)

(21) International Application Number:
PCT/US2016/050977

(22) International Filing Date:
9 September 2016 (09.09.2016)

(25) Filing Language: English

(26) Publication Language: English

(30) Priority Data:
62/216,969 10 September 2015 (10.09.2015) US

(71) Applicant: **MASSACHUSETTS INSTITUTE OF TECHNOLOGY** [US/US]; 77 Massachusetts Avenue, Cambridge, Massachusetts 02139 (US).

(72) Inventors: **ARTZI, Natalie**; 60 Gardner Road, Apt. 2, Brookline, Massachusetts 02445 (US). **CONDE, João**; 75 Cambridge Parkway, Apt. 405, Cambridge, Massachusetts 02142 (US). **OLIVA, Nuria**; 373 Highland Avenue, Apt. 213, Somerville, Massachusetts 02144 (US).

(74) Agents: **KING, Kevin W.** et al.; Sutherland Asbill & Brennan LLP, 999 Peachtree Street, NE, Atlanta, Georgia 30309-3996 (US).

(81) Designated States *(unless otherwise indicated, for every kind of national protection available)*: AE, AG, AL, AM, AO, AT, AU, AZ, BA, BB, BG, BH, BN, BR, BW, BY, BZ, CA, CH, CL, CN, CO, CR, CU, CZ, DE, DK, DM, DO, DZ, EC, EE, EG, ES, FI, GB, GD, GE, GH, GM, GT, HN, HR, HU, ID, IL, IN, IR, IS, JP, KE, KG, KN, KP, KR, KW, KZ, LA, LC, LK, LR, LS, LU, LY, MA, MD, ME, MG, MK, MN, MW, MX, MY, MZ, NA, NG, NI, NO, NZ, OM, PA, PE, PG, PH, PL, PT, QA, RO, RS, RU, RW, SA, SC, SD, SE, SG, SK, SL, SM, ST, SV, SY, TH, TJ, TM, TN, TR, TT, TZ, UA, UG, US, UZ, VC, VN, ZA, ZM, ZW.

(84) Designated States *(unless otherwise indicated, for every kind of regional protection available)*: ARIPO (BW, GH, GM, KE, LR, LS, MW, MZ, NA, RW, SD, SL, ST, SZ, TZ, UG, ZM, ZW), Eurasian (AM, AZ, BY, KG, KZ, RU, TJ, TM), European (AL, AT, BE, BG, CH, CY, CZ, DE, DK, EE, ES, FI, FR, GB, GR, HR, HU, IE, IS, IT, LT, LU, LV, MC, MK, MT, NL, NO, PL, PT, RO, RS, SE, SI, SK, SM, TR), OAPI (BF, BJ, CF, CG, CI, CM, GA, GN, GQ, GW, KM, ML, MR, NE, SN, TD, TG).

Declarations under Rule 4.17:

— *as to applicant's entitlement to apply for and be granted a patent (Rule 4.17(ii))*

[Continued on next page]

(54) Title: RNA TRIPLE HELIX STRUCTURES, COMPOSITIONS, AND METHODS

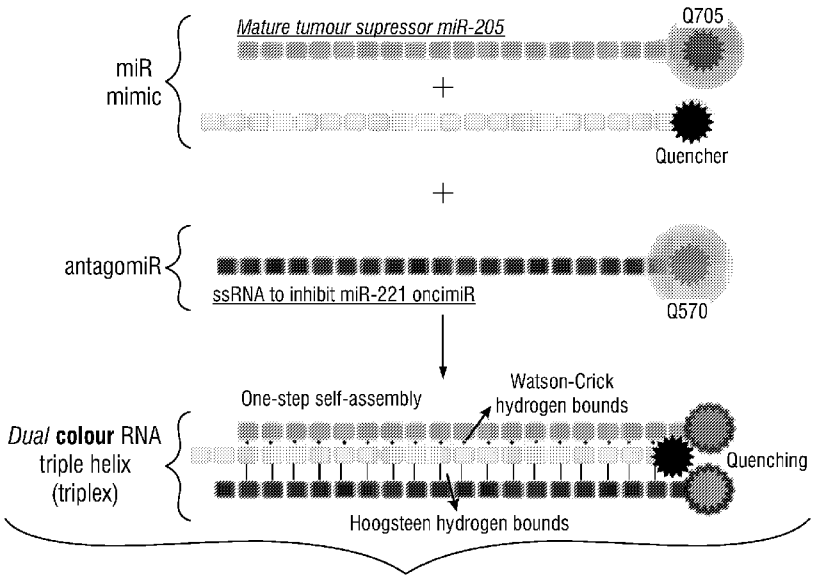

FIG. 1A

(57) Abstract: Provided herein are RNA triple helix structures. The RNA triple helix may be associated with a dendrimer to form an RNA triple helix-dendrimer conjugate, which may be applied to a biological tissue, such as a tumor. The RNA triple helix-dendrimer conjugate may be disposed in a hydrogel. The hydrogel may be applied to a biological tissue, such as a tumor. The hydrogel and/or dendrimer may control the release of the RNA triple helix. Methods of treating a biological tissue and kits also are provided.

WO 2017/044768 A1

— *as to the applicant's entitlement to claim the priority of the earlier application (Rule 4.17(iii))*

Published:

— *with international search report (Art. 21(3))*

— *before the expiration of the time limit for amending the claims and to be republished in the event of receipt of amendments (Rule 48.2(h))*

RNA TRIPLE HELIX STRUCTURES, COMPOSITIONS, AND METHODS

Cross-Reference to Related Application

This application claims priority to U.S. Provisional Patent Application No. 62/216,969, filed September 10, 2015, which is incorporated herein by reference.

Background

Fulfilling the potential of miRNA (miR) in cancer treatment has been difficult due to several disadvantages, including the lack of efficient delivery vehicles capable of releasing miRs to tumor cells. The delivery of miRs has been realized using inorganic nanoparticles (e.g. gold), liposomes, lipids, micelles, peptide nucleic acids (PNAs), packaging RNA (pRNA), and polymeric nanoparticles. However, miR dissociation from the vehicle, low vehicle stability, and/or inefficient targeting, have led to poor efficiency.

Therefore, improved delivery vehicles for miRNA are desirable, including those that address poor miR *in vivo* stability, non-specific biodistribution, modification of endogenous RNA machinery, and/or undesired side effects.

Brief Summary

Provided herein are compositions comprising an miRNA triple helix. The miRNA triple helices, in embodiments, comprise an miRNA sense oligonucleotide, an miRNA antisense oligonucleotide, and an antagomiRNA oligonucleotide. The miRNA sense oligonucleotide and the miRNA antisense oligonucleotide may be associated with each other by a plurality of Watson-Crick hydrogen bonds, and the antagomiRNA oligonucleotide and the miRNA sense oligonucleotide may be associated with each other by a plurality of Hoogsteen hydrogen bonds. The compositions, in some embodiments, further comprise a dendrimer having at least two branches with one or more surface groups, wherein the RNA triple helix is associated with the one or more surface groups of the dendrimer. In one embodiment, 100 % of the surface groups comprise at least one primary or secondary amine. The dendrimer and RNA triple helix may form an RNA triple helix-dendrimer conjugate, which may be a particulate material. The particulate material may aggregate to form a composition comprising a plurality of the aggregates.

Also provided herein are therapeutic compositions comprising [1] a hydrogel comprising a polymer and a first dendrimer, and [2] at least one RNA triple helix associated with a second dendrimer. The first dendrimer may have at least two branches with one or more surface groups, wherein at least a portion of the one or more surface groups comprise at least one primary or secondary amine. In embodiments, about 20 % to about 75 % of the surface groups of the first dendrimer include at least one primary or secondary amine. In a particular embodiment, about 25 % of the surface groups of the first dendrimer comprise at least one primary or secondary amine. In one embodiment, the second dendrimer comprises at least two branches with one or more surface groups, and 100 % of the surface groups of the second dendrimer comprise at least one primary or secondary amine.

Also provided herein are kits for making a therapeutic composition. The kits, in embodiments, comprise a first part which includes a first solution comprising a polymer component, wherein the polymer component comprises a polymer; and a second part which includes a second solution comprising a dendrimer component, wherein the dendrimer component comprises a first dendrimer having at least 2 branches with one or more surface groups, and a second dendrimer having a least 2 branches with one or more surface groups associated with an RNA triple helix. In one embodiment, 100 % of the surface groups of the second dendrimer comprise at least one primary or secondary amine. Also, about 20 % to about 75 % of the surface groups of the first dendrimer may include at least one primary or secondary amine. In a particular embodiment, about 25 % of the surface groups of the first dendrimer comprise at least one primary or secondary amine.

Also provided herein are methods for treating a biological tissue, for example, tissues including one or more tumors. The methods, in embodiments, comprise providing a first solution comprising a polymer component, wherein the polymer component comprises a polymer having three or more aldehyde groups; providing a second solution comprising a dendrimer component, wherein the dendrimer component comprises a first dendrimer having at least 2 branches with one or more surface groups, and a second dendrimer having a least 2 branches with one or more surface groups associated with an RNA triple helix; and combining the first and second solutions together to produce a therapeutic composition and contacting one or more biological tissues with the therapeutic composition. In one embodiment, 100 % of the surface groups of the second dendrimer comprise at least one primary or secondary amine. Also, about

20 % to about 75 % of the surface groups of the first dendrimer may include at least one primary or secondary amine. In a particular embodiment, about 25 % of the surface groups of the first dendrimer comprise at least one primary or secondary amine.

Also provided herein are methods comprising coating a tumor *in vivo* with an adhesive hydrogel composition. The adhesive hydrogel composition, in one embodiment, comprises an RNA triple helix. The RNA triple helix may comprise an miRNA mimic and an antagomiRNA. In embodiments, the adhesive hydrogel composition comprises a dendrimer associated with the RNA triple helix.

Brief Description of the Drawings

FIG. 1A is a schematic showing the self-assembly of one embodiment of an RNA triple helix.

FIG. 1B depicts the secondary structure of the RNA triple helix of **FIG. 1A**.

FIG. 1C depicts one embodiment of an RNA triple helix-dendrimer conjugate, and one embodiment of a hydrogel in which the RNA triple helix-dendrimer conjugate is disposed.

FIG. 2 depicts the effect of Mg^{2+} and Na^{+} on one embodiment of an RNA triple helix.

FIG. 3 is a high-resolution scanning electron microscope (SEM) image of the nanoparticles of RNA triple helix-dendrimer conjugates depicted at **FIG. 1C**.

FIG. 4 is a high-resolution SEM image of an aggregate of the nanoparticles of **FIG. 3**.

FIG. 5A is a high-resolution SEM image of the aggregates of **FIG. 4** embedded in one embodiment of a dextran-dendrimer hydrogel.

FIG. 5B is a high-resolution SEM image of the aggregates of **FIG. 4** embedded in one embodiment of a dextran-dendrimer hydrogel.

FIG. 5C is a high-resolution SEM image of the aggregates of **FIG. 4** embedded in one embodiment of a dextran-dendrimer hydrogel.

FIG. 6A is a table indicating the presence of certain embodiments of the RNA strands in the results depicted at **FIG. 6B**, **FIG. 6C**, and **FIG. 6D**.

FIG. 6B depicts the effect of temperature (25 °C) on the stability of the embodiments of the RNA strand combinations shown at **FIG. 6A**.

FIG. 6B depicts the effect of temperature (37 °C) on the stability of the embodiments of the RNA strand combinations shown at **FIG. 6A**.

FIG. 6B depicts the effect of temperature (65 °C) on the stability of the embodiments of the RNA strand combinations shown at **FIG. 6A**.

FIG. 7A depicts flow cytometry data which revealed the specific uptake of one embodiment of fluorescent RNA triple helix-dendrimer conjugate nanoparticles into MDA-MB-231 cells.

FIG. 7B depicts flow cytometry data which revealed the specific uptake of one embodiment of fluorescent RNA triple helix-dendrimer conjugate nanoparticles into MDA-MB-231 cells.

FIG. 7C depicts flow cytometry data which revealed the specific uptake of one embodiment of fluorescent RNA triple helix-dendrimer conjugate nanoparticles into MDA-MB-231 cells.

FIG. 7D depicts flow cytometry data which revealed the specific uptake of one embodiment of fluorescent RNA triple helix-dendrimer conjugate nanoparticles into MDA-MB-231 cells.

FIG. 8 depicts the expression of embodiments of RNA strands in breast cancer cells at different times.

FIG. 9 depicts cell viability at certain time periods.

FIG. 10 depicts the results of a wound closure assay.

FIG. 11 depicts the results of a clonogenic survival assay with crystal violet following treatment with embodiments of the RNA triple helix-dendrimer conjugates.

Detailed Description

Provided herein are RNA triple helix structures with improved stability, effectiveness, and/or tolerability. Embodiments of the RNA triple helices provided herein can improve cancer cells co-transfection efficiency. Also, the RNA triple helices provided herein can, in certain embodiments, modulate the expression of endogenous miRs in cancer *in vivo*. In one embodiment, the miRNA triple helix is a self-assembled dual-color RNA-triple-helix structure comprising two miRNAs, an miR mimic (tumor suppressor miRNA), and an antagomiR (oncomiR inhibitor)(**FIG. 1A** and **FIG. 1B**), which can provide the ability to synergistically abrogate tumors through delivery of one or both of the miRNAs.

The miRNA triple helices provided herein can be associated with a dendrimer to form RNA triple helix-dendrimer conjugates, which, in embodiments, can be stable triplex particles, including nanoparticles, as depicted schematically at **FIG. 1C**. The particles may aggregate to form aggregates. The aggregates and/or particles may be contacted with a polymer to form a hydrogel, which may act as an adhesive scaffold (*see* **FIG. 1C**). As a result, the hydrogel may adhere to natural tissue amines in a number of biological tissues, including tumors. A hydrogel and/or a dendrimer to which an RNA triple helix is conjugated can effect local and/or controlled release of the miRNA oligonucleotides of an RNA triple helix.

As described herein, the RNA triple helix-dendrimer conjugates are functional *in vitro* and *in vivo*, and certain embodiments have been demonstrated to achieve tumor shrinkage of up to about 90 % within two weeks after deployment in a triple-negative breast-cancer mouse model. Therefore, particular embodiments of the hydrogels containing RNA triple helix-dendrimer conjugates can be used as an efficient anticancer platform to locally modulate the expression of endogenous miRs in cancer.

RNA Triple Helix

Provided herein are compositions that include an RNA triple helix. The RNA triple helix, in embodiments, includes [1] an miRNA sense oligonucleotide, [2] an miRNA antisense oligonucleotide, and [3] an antagomiRNA oligonucleotide (oncomiR inhibitor). The miRNA sense oligonucleotide and miRNA antisense oligonucleotide may be part of an miRNA mimic (a tumor suppressor miRNA).

In embodiments, the molar ratio of the miRNA antisense oligonucleotide, miRNA sense oligonucleotide, and the antagomiRNA oligonucleotide in the RNA triple helix compositions is about (0.5—1.5):(0.5—1.5):(0.5—1. 5). In one embodiment, the molar ratio of the miRNA antisense oligonucleotide, miRNA sense oligonucleotide, and the antagomiRNA oligonucleotide in the RNA triple helix compositions is about (1):(0.5—1.5):(0.5—1. 5). In another embodiment, the molar ratio of the miRNA antisense oligonucleotide, miRNA sense oligonucleotide, and the antagomiRNA oligonucleotide in the RNA triple helix compositions is about (0.5—1.5):(1):(0.5—1. 5). In a further embodiment, the molar ratio of the miRNA antisense oligonucleotide, miRNA sense oligonucleotide, and the antagomiRNA oligonucleotide in the RNA triple helix compositions is about (0.5—1.5):(0.5—1.5):(1). In an additional embodiment, the molar ratio of the miRNA antisense oligonucleotide, miRNA sense

oligonucleotide, and the antagomiRNA oligonucleotide in the RNA triple helix compositions is about (1):(1):(0.5—1. 5). In yet another embodiment, the molar ratio of the miRNA antisense oligonucleotide, miRNA sense oligonucleotide, and the antagomiRNA oligonucleotide in the RNA triple helix compositions is about (0.5—1.5):(1):(1). In a still further embodiment, the molar ratio of the miRNA antisense oligonucleotide, miRNA sense oligonucleotide, and the antagomiRNA oligonucleotide in the RNA triple helix compositions is about (1):(0.5—1.5):(1). In some embodiments, the molar ratio of the miRNA antisense oligonucleotide, miRNA sense oligonucleotide, and the antagomiRNA oligonucleotide in the RNA triple helix compositions is about (1):(1):(1).

The miRNA oligonucleotides of the RNA triple helix may be associated with one another by a plurality of hydrogen bonds. The hydrogen bonds may include Watson-Crick hydrogen bonds, Hoogsteen hydrogen bonds, or a combination thereof. Not wishing to be bound by any particular theory, it is believed that the hydrogen bonds contribute, at least in part, to the formation of a stable RNA triple helix structure that is suitable for miR delivery.

In one embodiment, the miRNA sense oligonucleotide and the miRNA antisense oligonucleotide are associated with each other by a plurality of Watson-Crick hydrogen bonds. In another embodiment, the antagomiRNA oligonucleotide and the miRNA sense oligonucleotide are associated with each other by a plurality of Hoogsteen hydrogen bonds. In a further embodiment, the miRNA sense oligonucleotide and the miRNA antisense oligonucleotide are associated with each other by a plurality of Watson-Crick hydrogen bonds, and the antagomiRNA oligonucleotide and the miRNA sense oligonucleotide are associated with each other by a plurality of Hoogsteen hydrogen bonds.

As used herein, the phrase "associated with each other by a plurality of Watson-Crick hydrogen bonds" refers to two miRNA oligonucleotides that are attracted to each other by Watson-Crick hydrogen bonds that form between two or more bases of the first miRNA oligonucleotide and two or more bases of the second miRNA oligonucleotide. Although possible, not all of the bases of an miRNA oligonucleotide must participate in the Watson-Crick hydrogen bonding to satisfy the foregoing definition.

As used herein, the phrase "associated with each other by a plurality of Hoogsteen hydrogen bonds" refers to two miRNA oligonucleotides that are attracted to each other by Hoogsteen hydrogen bonds that form between two or more bases of the first miRNA

oligonucleotide and two or more bases of the second miRNA oligonucleotide. Although possible, not all of the bases of an miRNA oligonucleotide must participate in the Hoogsteen hydrogen bonding to satisfy the foregoing definition.

In embodiments, the RNA triple helix is a self-assembled structure. The RNA triple helix that may be formed by combining one or more miRNA oligonucleotides that form *Watson-Crick* and/or *Hoogsteen* hydrogen bonds. In certain embodiments, the triplex-forming oligonucleotides (TFO) bind antiparallel to the purine-rich strand in RNA, which requires no base protonation and exhibits pH independent binding.

In embodiments, the RNA triple helix induces further stacking within the tertiary structure domain, which may further improve structural stability.

In embodiments, the RNA triple helix may include substituents capable of reporting or detecting the formation of the RNA triple helix and/or the release of one or more therapeutic miRNAs. For example, the RNA triple helix can include one or more dyes, and one or more quenchers. In one embodiment, the central miRNA oligonucleotide of the RNA triple helix is substituted with a quencher at its ‘5 end, while the other two miRNA oligonucleotides are substituted with a dye at their 3’ ends. The dyes at the 3’ ends will be quenched upon formation of the RNA triple helix, and the quenching will cease if one or both of the dye-labeled miRNA oligonucleotides is separated from the RNA triple helix. Other configurations and combinations regarding dyes and quenchers are envisioned. In a particular embodiment, the RNA triple helix includes stable two-pair fluorescence resonance energy transfer (FRET) donor/quencher RNA oligonucleotides that are able to report the *in vivo* release of the miRNA oligonucleotides, which may occur upon conjugation to complementary targets.

In embodiments, the RNA triple helix is stable at a pH of about 4 to about 10. In some embodiments, the RNA triple helix is stable at a pH of about 5 to about 9. In one embodiment, the RNA triple helix is stable at a pH of about 5.5 to about 8.5. In another embodiment, the RNA triple helix is stable at a pH of about 6 to about 8. In a further embodiment, the RNA triple helix is stable at a pH of about 6.5 to about 7.5. In yet another embodiment, the RNA triple helix is stable at a pH of about 7.

In embodiments, the RNA triple helix is stable at a temperature of 70 °C or less. In another embodiment, the RNA triple helix is stable at a temperature of 65 °C or less. In a further embodiment, the RNA triple helix is stable at a temperature of 60 °C or less. In an additional

embodiment, the RNA triple helix is stable at a temperature of 55 °C or less. In a still further embodiment, the RNA triple helix is stable at a temperature of 50 °C or less. The stability of the RNA triple helix at various temperatures may be determined by the methods of Example 2 herein.

In embodiments, the RNA triple helix is stable at a pH of about 4 to about 10, and a temperature of 70 °C or less. In further embodiment, the RNA triple helix is stable at a pH of about 4 to about 10, and a temperature of 65 °C or less. In additional embodiments, the RNA triple helix is stable at a pH of about 4 to about 10, and a temperature of 60 °C or less. In one embodiment, the RNA triple helix is stable at a pH of about 4 to about 10, and a temperature of 55 °C or less. In another embodiment, the RNA triple helix is stable at a pH of about 4 to about 10, and a temperature of 50 °C or less.

In embodiments, the RNA triple helix is stable at a pH of about 5 to about 9, and a temperature of 70 °C or less. In further embodiment, the RNA triple helix is stable at a pH of about 5 to about 9, and a temperature of 65 °C or less. In additional embodiments, the RNA triple helix is stable at a pH of about 5 to about 9, and a temperature of 60 ° C or less. In one embodiment, the RNA triple helix is stable at a pH of about 5 to about 9, and a temperature of 55 °C or less. In another embodiment, the RNA triple helix is stable at a pH of about 5 to about 9, and a temperature of 50 °C or less.

In embodiments, the RNA triple helix is stable at a pH of about 5.5 to about 8.5, and a temperature of 70 °C or less. In further embodiment, the RNA triple helix is stable at a pH of about 5.5 to about 8.5, and a temperature of 65 °C or less. In additional embodiments, the RNA triple helix is stable at a pH of about 5.5 to about 8.5, and a temperature of 60 ° C or less. In one embodiment, the RNA triple helix is stable at a pH of about 5.5 to about 8.5, and a temperature of 55 °C or less. In another embodiment, the RNA triple helix is stable at a pH of about 5.5 to about 8.5, and a temperature of 50 °C or less.

In embodiments, the RNA triple helix is stable at a pH of about 6 to about 8, and a temperature of 70 °C or less. In further embodiment, the RNA triple helix is stable at a pH of about 6 to about 8, and a temperature of 65 °C or less. In additional embodiments, the RNA triple helix is stable at a pH of about 6 to about 8, and a temperature of 60 ° C or less. In one embodiment, the RNA triple helix is stable at a pH of about 6 to about 8, and a temperature of 55

°C or less. In another embodiment, the RNA triple helix is stable at a pH of about 6 to about 8, and a temperature of 50 °C or less.

miRNA Sense Oligonucleotide

In embodiments, the miRNA sense oligonucleotide includes from 20 to 40 nucleotides (nt). In one embodiment, the miRNA sense oligonucleotide includes from 25 to 35 nt. In another embodiment, the miRNA sense oligonucleotide includes from 26 to 30 nt. In a particular embodiment, the miRNA sense oligonucleotide includes 28 nt.

In embodiments, the miRNA sense oligonucleotide may be modified to include a quencher. The quencher may be used to verify triple helix formation when at least one of the other oligonucleotides of the triple helix is modified to include a dye. The quencher may be a BLACK HOLE QUENCHER® (LGC Biosearch Technologies, USA). The quencher may be placed at one end of the miRNA sense oligonucleotide, such as the 5' end. The 5' end may be appropriate when the 3' end of the antisense and/or the 3' end of the antagomiR oligonucleotides includes a dye.

In embodiments, the miRNA sense oligonucleotide may be modified to include a lipid. The lipid may be cholesterol. In one embodiment, the miRNA sense oligonucleotide includes a cholesterol molecule at its 3' end. Not wishing to be bound by any particular theory, it is believed that the inclusion of a lipid, such as a neutral lipid, can facilitate the permeation of cell membranes, improve co-transfection efficiency in vivo, and/or protect oligonucleotides from degradation.

In embodiments, the miRNA sense oligonucleotide is an miR-205 oligonucleotide. In one embodiment, the miRNA sense oligonucleotide is an miR-205 oligonucleotide that includes a lipid, such as a cholesterol, which may be at its 3' end. In a particular embodiment, the miRNA sense oligonucleotide is an miR-205 oligonucleotide that includes a quencher, such as a BLACK HOLE QUENCHER® (LGC Biosearch Technologies, USA), which may be at its 5' end. In a further embodiment, the miRNA sense oligonucleotide is an miR-205 oligonucleotide that includes a cholesterol at its 3' end, and a BLACK HOLE QUENCHER® (LGC Biosearch TECHNOLOGIES, USA) at its 5' end.

In embodiments, the miRNA sense oligonucleotide is an miR-200 oligonucleotide, including, but not limited to miR-200a, miR-200b, miR-200c, miR-141, and miR-429. Each of these miRNA sense oligonucleotides may be modified to include a lipid, such as a cholesterol,

and/or a quencher, such as a BLACK HOLE QUENCHER® (LGC Biosearch Technologies, USA). The lipid and/or quencher may be included at the ends of the miR-200 oligonucleotide. For example, the miRNA sense oligonucleotide may be an miR-200 oligonucleotide that is substituted at its 3' end with a lipid, such as a cholesterol, and at its 5' end with a quencher, such as a BLACK HOLE QUENCHER® (LGC Biosearch Technologies, USA).

miRNA Antisense Oligonucleotide

In embodiments, the miRNA antisense oligonucleotide and miRNA sense oligonucleotide are an miRNA mimic (tumor suppressor miRNA), such as a mature tumor suppressor miRNA-205 (*see* **FIG. 1A** and **FIG. 1B**). The miRNA mimic may be a mature miRNA duplex comprising both sense and antisense strands.

In embodiments, the miRNA antisense oligonucleotide includes from 20 to 40 nucleotides (nt). In one embodiment, the miRNA antisense oligonucleotide includes from 25 to 35 nt. In another embodiment, the miRNA antisense oligonucleotide includes from 26 to 30 nt. In a particular embodiment, the miRNA antisense oligonucleotide includes 28 nt.

In embodiments, the miRNA antisense oligonucleotide may be modified to include a dye. The dye may be used to verify triple helix formation when at least one of the other oligonucleotides of the triple helix is modified to include a quencher. The dye may be a near infrared (NIR) dye, such as QUASAR® 705 (LGC Biosearch Technologies, USA). The dye may be placed at one end of the miRNA antisense oligonucleotide, such as the 3' end. The 3' end may be appropriate when the 5' end of the miRNA sense oligonucleotide and/or the 3' end of the antagomiR oligonucleotide includes a quencher or a dye, respectively.

AntagomiRNA Oligonucleotide

In embodiments, the antagomiRNA oligonucleotide may be a synthetic single-stranded RNA (ssRNA) used to inhibit an omcomiRNA.

In embodiments, the antagomiRNA oligonucleotide includes from 20 to 40 nucleotides (nt). In one embodiment, the antagomiRNA oligonucleotide includes from 25 to 35 nt. In another embodiment, the antagomiRNA oligonucleotide includes from 28 to 32 nt. In a particular embodiment, the antagomiRNA oligonucleotide includes 30 nt.

In embodiments, the antagomiRNA oligonucleotide may be modified to include a dye. The dye may be used to verify triple helix formation when at least one of the other oligonucleotides of the triple helix is modified to include a quencher. The dye may be a near

infrared (NIR) dye, such as QUASAR® 570 (LGC Biosearch Technologies, USA). The dye may be placed at one end of the antagomiRNA oligonucleotide, such as the 3' end. The 3' end may be appropriate when the 5' end of the miRNA sense oligonucleotide and/or the 3' end of the miRNA antisense oligonucleotide includes a quencher or a dye, respectively.

In one embodiment, the antagomiRNA oligonucleotide is an antagomiR-221 oligonucleotide.

Formation of the RNA Triple Helix

In embodiments, the RNA triple helix is formed by contacting the miRNA oligonucleotides of the triple helix in an appropriate medium. The medium may be an incubation buffer. In one embodiment, the incubation buffer is a tris(hydroxymethyl)aminomethane (Tris) buffer (pH 7).

The Tris buffer may be supplemented with one or more supplements, such as $MgCl_2$, spermine, $CuSO_4$, or a combination thereof. In one embodiment, the Tris buffer is a 10 mM Tris buffer supplemented with $MgCl_2$, such as 10 mM $MgCl_2$. In another embodiment, the Tris buffer is a 10 mM Tris buffer supplemented with spermine, such as 1 mM spermine. In a further embodiment, the Tris buffer is a 10 mM Tris buffer supplemented with $CuSO_4$, such as 0.8 mM $CuSO_4$. In some embodiments, the Tris buffer is a 10 mM Tris buffer supplemented with $MgCl_2$, such as 10 mM $MgCl_2$, and spermine, such as 1 mM spermine. In further embodiments, the Tris buffer is a 10 mM Tris buffer supplemented with $MgCl_2$, such as 10 mM $MgCl_2$, and $CuSO_4$, such as 0.8 mM $CuSO_4$. In yet another embodiment, the Tris buffer is a 10 mM Tris buffer supplemented with $CuSO_4$, such as 0.8 mM $CuSO_4$, and spermine, such as 1 mM spermine. In still additional embodiments, the Tris buffer is a 10 mM Tris buffer supplemented with 10 mM $MgCl_2$, 1 mM spermine, and 0.8 mM $CuSO_4$.

Not wishing to be bound by any particular theory, it is believed that the supplemental copper ions may favor the intercalation of the nitrogen atoms in the minor groove of the RNA triple helix or triplex where copper binding occurs (*see*, *e.g.*, Francois, J.C. et al. *Proceedings of the National Academy of Sciences of the United States of America*, **86**, 9702-9706 (1989)).

Not wishing to be bound by any particular theory, it is believed that the spermine, as a natural polyamine, may improve triplex formation by reducing the electrostatic repulsive forces between the negatively charged phosphate backbones of the RNA strands (*see*, *e.g.*, Tung, C.H. et al. *Nucleic Acids Research* **21** 5489-5494 (1993)).

Not wishing to be bound by any particular theory, it is believed that Mg^{2+} may promote RNA triple helix formation due to charge neutralization. Moreover, Mg^{2+} is believed to bind to the phosphate groups of the RNA triple helix, which may reduce the repulsion between the three phosphate frameworks, thereby increasing the efficiency of the triple-helix formation.

Contrary to the Mg^{2+} effect and not wishing to be bound by any particular theory, Na^{+} is believed to be a possible inhibitor of DNA triple helix formation (*see* **FIG. 2**). The hindering effect of Na^{+} may be explained by the polyelectrolyte effect: a high concentration of Na^{+} is believed to lower the population of Mg^{2+} in the vicinity of DNA or RNA, thereby decreasing the probability of triple helix formation. It also is believed that Na^{+} had the ability to form undesirable dimers and tetramers, thereby decreasing the efficiency of triple helix formation.

In embodiments, the RNA triple helix is formed by [1] contacting the miRNA oligonucleotides in an appropriate medium, such as a Tris buffer, which may be supplemented as provided herein, and [2] heating the medium to a temperature of about 60 to about 100 °C, about 70 to about 90 °C, or about 80 °C. The medium may be heated for about 1 to about 10 minutes, from about 3 to about 7 minutes, or about 5 minutes. The medium may then be cooled to a temperature of about 1 to about 10 °C, from about 2 to about 6 ° C, or about 4 °C.

RNA Triple Helix – Dendrimer Conjugates

The RNA triple helix may be associated with a dendrimer to form an RNA triple helix-dendrimer conjugate. The dendrimer of the RNA triple helix-dendrimer conjugate may allow the release of the RNA triple helix and/or one or more miRNAs of the RNA triple helix from the RNA triple helix-dendrimer conjugates to be controlled.

The RNA triple helix-dendrimer conjugate may be a particulate material. The particulate material may be substantially spherical. In one embodiment, the particulate material comprises nanoparticles. In a further embodiment, the particulate material comprises substantially spherical nanoparticles. The nanoparticles may have an average largest dimension of about 30 to about 80 nm, from about 40 to about 70 nm, or from about 50 to about 60 nm. The average largest dimension may be determined by SEM images or X-ray diffraction, and is the diameter when the particulate material is substantially spherical.

The RNA triple helix-dendrimer conjugates may be a particulate material that forms aggregates. The aggregates of the particulate material may be substantially spherical. The aggregates of the particulate material may be a microscale material. The microscale material

may be substantially spherical. The aggregates may have an average largest dimension of about 1 to about 10 μm, from about 2 to about 8 μm, from about 3 to about 5 μm, or from about 3 to about 4 μm. The average largest dimension may be determined by SEM images or X-ray diffraction, and is the diameter when the aggregates are substantially spherical.

In one embodiment, the RNA triple helix-dendrimer conjugates are in the form of a particulate material, aggregates of a particulate material, or a combination thereof. In another embodiment, the RNA triple helix-dendrimer conjugates are in the form of aggregates of a particulate material. In yet another embodiment, the RNA triple helix-dendrimer conjugates are in the form of a particulate material. In a still further embodiment, a first portion of the RNA triple helix-dendrimer conjugates are in the form of a particulate material, and a second portion of the RNA triple helix-dendrimer conjugates are in the form of aggregates of a particulate material.

Therefore, the RNA triple helices provided herein can be provided at various scales, including nanoscale, microscale, and macroscale. In one embodiment, an RNA triple helix-dendrimer conjugates can be provided as nanoparticles. One example of nanoparticles of an RNA triple helix-dendrimer conjugate is depicted at **FIG. 3**, which is a high-resolution SEM image of the RNA triple helix-dendrimer conjugate nanoparticles of **FIG. 1C**, which have an average largest dimension of about 50 nm to about 60 nm. In another embodiment, RNA triple helix-dendrimer conjugates can be provided as microparticles, which may be aggregates of the RNA triple helix-dendrimer conjugate nanoparticles. One example of a microscale aggregate is depicted at **FIG. 4**, which is a high-resolution SEM image of an aggregate of the nanoparticles of RNA triple helix-dendrimer conjugates of **FIG. 3**, and the aggregate has a largest dimension of about 3 μm to about 4 μm. In a further embodiment, RNA triple helix-dendrimer conjugates can be provided at the macroscale (> 1 mm) when embedded in a hydrogel, as shown at **FIG. 5A, FIG. 5B,** and **FIG. 5C**, which are high-resolution SEM images of the aggregates of **FIG. 4** embedded in one embodiment of a dextran-dendrimer hydrogel.

In the RNA triple helix-dendrimer conjugates, the RNA triple helix may be associated with the dendrimer through one or more attractive forces. The attractive forces may include an interaction between the phosphates of the miRNA oligonucleotides and the surface groups of the dendrimer. The surface groups may have a cationic character. In one embodiment, a cationic surface of the dendrimer provides an easy platform for conjugating the dendrimer with miRNA

oligonucleotides via electrostatic interactions between the cationic surface groups, such as positively charged terminal amines from PAMAM dendrimers, and the negatively charged RNA phosphate of the miRNA oligonucleotides.

In embodiments, the dendrimer of the RNA triple helix-dendrimer conjugates comprises a dendrimer having amines on at least a portion of its surface groups, which are commonly referred to as "terminal groups" or "end groups." The dendrimer may have amines on from about 75 % to 100 % of its surface groups, from about 80 % to about 100 % of its surface groups, from about 85 % to about 100 % of its surface groups, from about 90 % to about 100 % of its surface groups, from about 95 % to about 100 % of its surface groups, or from about 98 % to about 100 % of its surface groups. In some embodiments, the dendrimer has amines on 100 % of its surface groups. As used herein, the term "dendrimer" refers to any compound with a polyvalent core covalently bonded to two or more dendritic branches. In some embodiments, the polyvalent core is covalently bonded to three or more dendritic branches. In one embodiment, the amines are primary amines. In another embodiment, the amines are secondary amines. In yet another embodiment, one or more surface groups have at least one primary and at least one secondary amine.

In one embodiment, the dendrimer of the RNA triple helix-dendrimer conjugates extends through at least 2 generations. In another embodiment, the dendrimer of the RNA triple helix-dendrimer conjugates extends through at least 3 generations. In yet another embodiment, the dendrimer of the RNA triple helix-dendrimer conjugates extends through at least 4 generations. In still another embodiment, the dendrimer of the RNA triple helix-dendrimer conjugates extends through at least 5 generations. In a further embodiment, the dendrimer of the RNA triple helix-dendrimer conjugates extends through at least 6 generations. In still a further embodiment, the dendrimer of the RNA triple helix-dendrimer conjugates extends through at least 7 generations.

In one embodiment, the dendrimer of the RNA triple helix-dendrimer conjugates has a molecular weight of from about 1,000 to about 1,000,000 Daltons. In a further embodiment, the dendrimer of the RNA triple helix-dendrimer conjugates has a molecular weight of from about 3,000 to about 120,000 Daltons. In another embodiment, the dendrimer of the RNA triple helix-dendrimer conjugates has a molecular weight of from about 10,000 to about 100,000 Daltons. In yet another embodiment, the dendrimer of the RNA triple helix-dendrimer conjugates has a molecular weight of from about 20,000 to about 40,000 Daltons. Unless specified otherwise, the

"molecular weight" of the dendrimer of the RNA triple helix-dendrimer conjugates refers to the number average molecular weight.

Generally, the dendrimer of the RNA triple helix-dendrimer conjugates may be made using any known methods. In one embodiment, the dendrimer of the RNA triple helix-dendrimer conjugates is made by oxidizing a starting dendrimer having surface groups comprising at least one hydroxyl group so that at least a portion of the surface groups comprise at least one amine. In another embodiment, the dendrimer of the RNA triple helix-dendrimer conjugates is made by oxidizing a starting generation 5 (G5) dendrimer having surface groups comprising at least one hydroxyl group so that at least about 75 % to about 100 % of the surface groups comprise at least one amine.

In one embodiment, the dendrimer of the RNA triple helix-dendrimer conjugates is a poly(amidoamine)-derived (PAMAM) dendrimer. In another embodiment, the dendrimer of the RNA triple helix-dendrimer conjugates is a G5 PAMAM-derived dendrimer. In yet another embodiment, the dendrimer of the RNA triple helix-dendrimer conjugates is a G5 PAMAM-derived dendrimer having primary amines on about 75 to about 100 % of the dendrimer's surface groups. In a still further embodiment, the dendrimer of the RNA triple helix-dendrimer conjugates is a G5 PAMAM-derived dendrimer having primary amines on about 80 to about 100 % of the dendrimer's surface groups. In yet another embodiment, the dendrimer of the RNA triple helix-dendrimer conjugates is a G5 PAMAM-derived dendrimer having primary amines on about 90 to about 100 % of the dendrimer's surface groups. In a still further embodiment, the dendrimer of the RNA triple helix-dendrimer conjugates is a G5 PAMAM-derived dendrimer having primary amines on 100 % of the dendrimer's surface groups.

In one embodiment, the dendrimer of the RNA triple helix-dendrimer conjugates is a poly(propyleneimine)-derived dendrimer.

Dendrimer Component of Hydrogel

In embodiments, an RNA triple helix and/or an RNA triple helix-dendrimer conjugate is disposed in a hydrogel. The hydrogel may comprise a polymer component and a dendrimer component. In one embodiment, an RNA triple helix is disposed in the hydrogel. The RNA triple helix may be substantially evenly dispersed in the hydrogel. In another embodiment, an RNA triple helix-dendrimer conjugate is disposed in a hydrogel. The RNA triple helix-dendrimer conjugate may be substantially evenly dispersed in the hydrogel. In yet another

embodiment, an RNA triple helix and an RNA triple helix-dendrimer conjugate is disposed in a hydrogel. At least one of the RNA triple helix and RNA triple helix-dendrimer conjugate may be substantially evenly dispersed in the hydrogel.

In embodiments, the dendrimer component of the hydrogel comprises a dendrimer that includes one or more surface groups capable of reacting with a polymer group. In another embodiment, the dendrimer component of the hydrogel comprises a first dendrimer that includes one or more surface groups capable of reacting with a polymer group, and a second dendrimer that is associated with an RNA triple helix. The first dendrimer and the second dendrimer that is associated with an RNA triple helix, in a particular embodiment, have substantially identical structures. In another embodiment, the first dendrimer and the second dendrimer that is associated with an RNA triple have different structures. The first dendrimer is referred to herein as the "hydrogel-forming dendrimer." Although the first dendrimer is referred to as a "hydrogel-forming dendrimer," the use of this phrase is not intended to convey that the second dendrimer does not participate, at least to some degree, in hydrogel formation, although it is possible that the second dendrimer may not participate in hydrogel formation, at least in some embodiments. In particular embodiments herein, both the first dendrimer and the second dendrimer contribute to the formation of a hydrogel. In other embodiments, the first dendrimer contributes to hydrogel formation, and the second dendrimer does not substantially contribute to hydrogel formation.

In embodiments, the hydrogel-forming dendrimer has amines on at least a portion of its surface groups, which are commonly referred to as "terminal groups" or "end groups." The hydrogel-forming dendrimer may have amines on from about 20 % to 100 % of its surface groups. In some embodiments, the hydrogel-forming dendrimer has amines on about 20 % to about 80 % of its surface groups. In one embodiment, the hydrogel-forming dendrimer has amines on less than 75 % of its surface groups. In a particular embodiment, the hydrogel-forming dendrimer has amines of about 20 % to about 75 % of its surface groups. In a particular embodiment, the hydrogel-forming dendrimer has amines of about 20 % to about 60 % of its surface groups. In a certain embodiment, the hydrogel-forming dendrimer has amines of about 20 % to about 50 % of its surface groups. In another embodiment, the hydrogel-forming dendrimer has amines of about 20 % to about 50 % of its surface groups. In a further embodiment, the hydrogel-forming dendrimer has amines of about 20 % to about 40 % of its

surface groups. In yet another embodiment, the hydrogel-forming dendrimer has amines of about 20 % to about 30 % of its surface groups. In a still further embodiment, the hydrogel-forming dendrimer has amines on about 25 % of its surface groups.

In one embodiment, the hydrogel-forming dendrimer extends through at least 2 generations. In another embodiment, the hydrogel-forming dendrimer extends through at least 3 generations. In yet another embodiment, the hydrogel-forming dendrimer extends through at least 4 generations. In still another embodiment, the hydrogel-forming dendrimer extends through at least 5 generations. In a further embodiment, the hydrogel-forming dendrimer extends through at least 6 generations. In still a further embodiment, the hydrogel-forming dendrimer extends through at least 7 generations.

In one embodiment, the hydrogel-forming dendrimer has a molecular weight of from about 1,000 to about 1,000,000 Daltons. In a further embodiment, the hydrogel-forming dendrimer has a molecular weight of from about 3,000 to about 120,000 Daltons. In another embodiment, the hydrogel-forming dendrimer has a molecular weight of from about 10,000 to about 100,000 Daltons. In yet another embodiment, the hydrogel-forming dendrimer has a molecular weight of from about 20,000 to about 40,000 Daltons. Unless specified otherwise, the "molecular weight" of the hydrogel-forming dendrimer refers to the number average molecular weight.

Generally, the hydrogel-forming dendrimer may be made using any known methods. In one embodiment, the hydrogel-forming dendrimer is made by oxidizing a starting dendrimer having surface groups comprising at least one hydroxyl group so that at least a portion of the surface groups comprise at least one amine. In another embodiment, the hydrogel-forming dendrimer is made by oxidizing a starting generation 5 (G5) dendrimer having surface groups comprising at least one hydroxyl group so that at least a portion of the surface groups comprise at least one amine. In yet another embodiment, the hydrogel-forming dendrimer is made by oxidizing a starting G5 dendrimer having surface groups comprising at least one hydroxyl group so that about 25 % of the surface groups comprise at least one amine. In a particular embodiment, the hydrogel-forming dendrimer is a G5 dendrimer having primary amines on about 25 % of the dendrimer's surface groups.

In one embodiment, the hydrogel-forming dendrimer is a poly(amidoamine)-derived (PAMAM) dendrimer. In another embodiment, the hydrogel-forming dendrimer is a G5

PAMAM-derived dendrimer. In yet another embodiment, the hydrogel-forming dendrimer is a G5 PAMAM-derived dendrimer having primary amines on about 25 % of the dendrimer's surface groups.

In one embodiment, the hydrogel-forming dendrimer is a poly(propyleneimine)-derived dendrimer.

In certain embodiments, the dendrimer component is combined with a liquid to form a dendrimer component solution. In one embodiment, the dendrimer component solution is an aqueous solution. In one embodiment, the solution comprises water, phosphate buffer saline (PBS), Dulbecco's Modified Eagle's Medium (DMEM), or any combination thereof. In one embodiment, the dendrimer component concentration in the dendrimer component solution is about 5 % to about 25 % by weight. In another embodiment, the dendrimer component concentration in the dendrimer component solution is about 10 % to about 20 % by weight. In a further embodiment, the dendrimer component concentration in the dendrimer component solution is about 11 % to about 15 % by weight.

In embodiments, the dendrimer component comprises an RNA triple helix, and the concentration of the RNA triple helix in the dendrimer component solution is about 0.1 to about 1.0 micromolar. In further embodiments, the dendrimer component comprises a first dendrimer that includes one or more surface groups capable of reacting with a polymer group, and a second dendrimer that is associated with an RNA triple helix, and the concentration of the second dendrimer in the dendrimer component solution is about 0.01 to about 5 mg/mL, and the concentration of the RNA triple helix is about 0.1 to about 1.0 micromolar. In one embodiment, the dendrimer component comprises a first dendrimer that includes one or more surface groups capable of reacting with a polymer group, and a second dendrimer that is associated with an RNA triple helix, and the concentration of the second dendrimer in the dendrimer component solution is about 0.05 mg/mL, and the concentration of the RNA triple helix is about 1.0 micromolar.

In some instances, the dendrimer component or dendrimer component solution further includes one or more additives. Generally, the amount of additive may vary depending on the application, tissue type, concentration of the dendrimer component solution, the type of dendrimer component, concentration of the polymer component solutions, and/or the type of polymer component. Example of suitable additives include, but are not limited to, pH modifiers,

thickeners, antimicrobial agents, colorants, surfactants, and radio-opaque compounds. Specific examples of these types of additives are described herein. In one embodiment, the dendrimer component solution comprises a foaming additive.

In particular embodiments, the dendrimer component or dendrimer component solution includes one or more drugs. Alternatively, or in addition, the polymer component or polymer component solution includes one or more drugs. In such embodiments, the hydrogel may serve as a matrix material for controlled release of the one or more drugs. The drug may be essentially any drug suitable for local, regional, or systemic administration from a quantity of the hydrogel that has been applied to one or more tissue sites in a patient.

In other particular embodiments, the dendrimer component or dendrimer component solution includes one or more cells. Alternatively, or in addition, the polymer component or polymer component solution includes one or more cells.

In certain embodiments, the pH modifier is an acidic compound. Examples of acidic pH modifiers include, but are not limited to, carboxylic acids, inorganic acids, and sulfonic acids. In other embodiments, the pH modifier is a basic compound. Examples of basic pH modifiers include, but are not limited to, hydroxides, alkoxides, nitrogen-containing compounds other than primary and secondary amines, basic carbonates, and basic phosphates.

Generally, the thickener may be selected from any known viscosity-modifying compounds, including, but not limited to, polysaccharides and derivatives thereof, such as starch or hydroxyethyl cellulose.

Generally, the surfactant may be any compound that lowers the surface tension of water. In one embodiment, the surfactant is an ionic surfactant—for example, sodium lauryl sulfate. In another embodiment, the surfactant is a neutral surfactant. Examples of neutral surfactants include, but are not limited to, polyoxyethylene ethers, polyoxyethylene esters, and polyoxyethylene sorbitan.

In one embodiment, the radio-opaque compound is barium sulfate, gold particles, or a combination thereof.

Polymer Component

Generally, the polymer component includes a polymer with one or more functional groups capable of reacting with one or more functional groups on a biological tissue and/or one or more functional groups on a dendrimer of the dendrimer component.

In certain embodiments, the polymer is at least one polysaccharide. In these embodiments, the at least one polysaccharide may be linear, branched, or have both linear and branched sections within its structure. Generally, the at least one polysaccharide may be natural, synthetic, or modified—for example, by cross-linking, altering the polysaccharide's substituents, or both. In one embodiment, the at least one polysaccharide is plant-based. In another embodiment, the at least one polysaccharide is animal-based. In yet another embodiment, the at least one polysaccharide is a combination of plant-based and animal-based polysaccharides. Non-limiting examples of polysaccharides include, but are not limited to, dextran, chitin, starch, agar, cellulose, hyaluronic acid, or a combination thereof.

In certain embodiments, the at least one polymer has a molecular weight of from about 1,000 to about 1,000,000 Daltons. In one embodiment, the at least one polymer has a molecular weight of from about 5,000 to about 15,000 Daltons. Unless specified otherwise, the "molecular weight" of the polymer refers to the number average molecular weight.

In some embodiments, the polymer is functionalized so that its structure includes one or more functional groups that will react with one or more functional groups on a biological tissue and/or one or more functional groups on a dendrimer of the dendrimer component. In other embodiments, the polymer is functionalized so that its structure includes three or more functional groups that will react with one or more functional groups on a biological tissue and/or one or more functional groups on a dendrimer of the dendrimer component. In one embodiment, the functional group incorporated into the polymer's structure is aldehyde.

In certain embodiments, the polymer's degree of functionalization is adjustable. The "degree of functionalization" generally refers to the number or percentage of groups on the polymer that are replaced or converted to the desired one or more functional groups. The one or more functional groups, in particular embodiments, include aldehydes. In one embodiment, the degree of functionalization is adjusted based on the type of tissue to which the hydrogel is applied, the concentration(s) of the components, and/or the type of polymer or dendrimer used in the hydrogel. In one embodiment, the degree of functionalization is from about 10 % to about 75 %. In another embodiment, the degree of functionalization is from about 15 % to about 50 %. In yet another embodiment, the degree of functionalization is from about 20 % to about 30 %.

In one embodiment, the polymer is a polysaccharide having from about 10 % to about 75 % of its hydroxyl groups converted to aldehydes. In another embodiment, the polymer is a

polysaccharide having from about 20 % to about 50 % of its hydroxyl groups converted to aldehydes. In yet another embodiment, the polymer is a polysaccharide having from about 10 % to about 30 % of its hydroxyl groups converted to aldehydes.

In one embodiment, the polymer is dextran with a molecular weight of about 10 kDa. In another embodiment, the polymer is dextran having about 50 % of its hydroxyl group converted to aldehydes. In a further embodiment, the polymer is dextran with a molecular weight of about 10 kDa and about 50 % of its hydroxyl groups converted to aldehydes.

In some embodiments, a polysaccharide is oxidized to include a desired percentage of one or more aldehyde functional groups. Generally, this oxidation may be conducted using any known means. For example, suitable oxidizing agents include, but are not limited to, periodates, hypochlorites, ozone, peroxides, hydroperoxides, persulfates, and percarbonates. In one embodiment, the oxidation is performed using sodium periodate. Typically, different amounts of oxidizing agents may be used to alter the degree of functionalization.

In certain embodiments, the polymer component is combined with a liquid to form a polymer component solution. In one embodiment, the polymer component solution is an aqueous solution. In one embodiment, the solution comprises water, PBS, DMEM, or any combination thereof.

Generally, the polymer component solution may have any suitable concentration of polymer component. In one embodiment, the polymer component concentration in the polymer component solution is about 5 % to about 40 % by weight. In another embodiment, the polymer component concentration in the polymer component solution is about 5 % to about 30 % by weight. In yet another embodiment, the polymer component concentration in the polymer component solution is about 5 % to about 25 % by weight. Typically, the concentration may be tailored and/or adjusted based on the particular application, tissue type, and/or the type and concentration of dendrimer component used.

The polymer component or polymer component solution may also include one or more additives. In one embodiment, the additive is compatible with the polymer component. In another embodiment, the additive does not contain primary or secondary amines. Generally, the amount of additive varies depending on the application, tissue type, concentration of the polymer component solution, the type of polymer component and/or dendrimer component. Examples of suitable additives, include, but are not limited to, pH modifiers, thickeners, antimicrobial agents,

colorants, surfactants, radio-opaque compounds, and the other additives described herein. In other embodiments, the polymer component solution comprises a foaming agent.

In certain embodiments, the pH modifier is an acidic compound. Examples of acidic pH modifiers include, but are not limited to, carboxylic acids, inorganic acids, and sulfonic acids. In other embodiments, the pH modifier is a basic compound. Examples of basic pH modifiers include, but are not limited to, hydroxides, alkoxides, nitrogen-containing compounds other than primary and secondary amines, basic carbonates, and basic phosphates.

Generally, the thickener may be selected from any known viscosity-modifying compounds, including, but not limited to, polysaccharides and derivatives thereof, such as starch or hydroxyethyl cellulose.

Generally, the surfactant may be any compound that lowers the surface tension of water. In one embodiment, the surfactant is an ionic surfactant—for example, sodium lauryl sulfate. In another embodiment, the surfactant is a neutral surfactant. Examples of neutral surfactants include, but are not limited to, polyoxyethylene ethers, polyoxyethylene esters, and polyoxyethylene sorbitan.

In one embodiment, the radio-opaque compound is barium sulfate, gold particles, or a combination thereof.

In particular embodiments, the polymer component or polymer component solution includes one or more drugs. In such embodiments, the hydrogel may serve as a matrix material for controlled release of drug. The drug may be essentially any drug suitable for local, regional, or systemic administration from a quantity of the hydrogel that has been applied to one or more tissue sites in a patient.

In other particular embodiments, the polymer component or polymer component solution includes one or more cells. For example, the hydrogel may serve as a matrix material for delivering cells to a tissue site at which the hydrogel has been applied.

Hydrogel Formation

Generally, the hydrogels described herein may be formed by combining the polymer component or polymer component solution, and the dendrimer component or dendrimer component solution in any manner. In some embodiments, the polymer component or polymer component solution, and the dendrimer component or dendrimer component solution are combined before contacting a biological tissue with the hydrogel. In other embodiments, the

polymer component or polymer component solution, and the dendrimer component or dendrimer component solution are combined, in any order, on a biological tissue. Therefore, the combining and contacting steps may be performed simultaneously or in any order. In further embodiments, the polymer component or polymer component solution is applied to a first biological tissue, the dendrimer component or dendrimer component solution is applied to a second biological tissue, and the first and second biological tissues are contacted. In still a further embodiment, the polymer component or polymer component solution is applied to a first region a biological tissue, the dendrimer component or dendrimer component solution is applied to a second region of a biological tissue, and the first and second regions are contacted.

In embodiments, the hydrogel comprises an RNA triple helix and/or one or more RNA triple helix-dendrimer conjugates. Generally, the RNA triple helix and/or one or more RNA triple helix-dendrimer conjugates may be combined with or added to a component and/or component solution prior to hydrogel formation, or, alternatively or additionally, the RNA triple helix and/or one or more RNA triple helix-dendrimer conjugates may be added to a hydrogel during or after hydrogel formation and/or curing. In one embodiment, the RNA triple helix and/or one or more RNA triple-helix dendrimer conjugates is combined with or added to the dendrimer component or the dendrimer component solution prior to hydrogel formation. In one embodiment, the RNA triple helix and /or one or more RNA triple-helix dendrimer conjugates is disposed in a hydrogel during and/or after formation and/or curing of the hydrogel.

Generally, the hydrogels may be applied to one or more biological tissues as an adhesive, sealant, and/or treatment. In one embodiment, the biological tissue includes a tumor. In another embodiment, the biological tissue includes a tumor, tissue adjacent to a tumor, or a combination thereof. The phrase "applied to," as used herein, refers to the placement of a hydrogel on, in, and/or adjacent to a biological tissue. The one or more biological tissues may be diseased, damaged (*e.g.*, dissected), healthy, or some combination thereof. In one embodiment, the hydrogel is applied to one or more biological tissues as an adhesive. In another embodiment, the hydrogel is applied to one or more biological tissues as a sealant. In a further embodiment, the hydrogel is applied to one or more biological tissues as a treatment. In an additional embodiment, the hydrogel is applied to one or more biological tissues as an adhesive and sealant. In still another embodiment, the hydrogel is applied to one or more biological tissues as an adhesive and treatment. In yet another embodiment, the hydrogel is applied to one or more

biological tissues as a sealant and treatment. In a still further embodiment, the hydrogel is applied to one or more biological tissues as an adhesive, sealant, and treatment.

The hydrogel may be applied to the biological tissue using any suitable tool and methods. Non-limiting examples include the use of syringes or spatulas. Double barrel syringes with rigid or flexible discharge tips, and optional extension tubes, known in the art are envisioned.

As used herein, the hydrogel is a "treatment" when it improves the response of at least one biological tissue to which it is applied. In some embodiments, the improved response is lessening tumor growth, lessening tumor size, lessening overall inflammation, improving the specific response at the wound site/ interface of the tissue and hydrogel, enhancing healing, or a combination thereof. As used herein, the phrase "lessening tumor growth" refers to a decrease in the rate of tumor growth or the temporary or permanent cessation of tumor growth. As used herein, the phrase "lessening tumor size" refers to a decrease in one or more dimensions of a tumor. As used herein, the phrase "lessening overall inflammation" refers to an improvement of histology scores that reflect the severity of inflammation. As used herein, the phrase "improving the specific response at the wound site/interface of the tissue and hydrogel" refers to an improvement of histology scores that reflect the severity of serosal neutrophils. As used herein, the phrase "enhancing healing" refers to an improvement of histology scores that reflect the severity of serosal fibrosis.

After contacting one or more biological tissues, the formulation may be allowed adequate time to cure or gel. When the hydrogel "cures" or "gels," as those terms are used herein, it means that the reactive groups on the polymer component, dendrimer component, and one or more biological tissues have undergone one or more reactions. Not wishing to be bound by any particular theory, it is believed that the hydrogels described herein are effective because the polymer component reacts with both the dendrimer component and the surface of the biological tissues. In certain embodiments, the polymer component's aldehyde functional groups react with the amines on a dendrimer of the dendrimer component and the biological tissues to form imine bonds. In these embodiments, it is believed that the amines on the dendrimer component react with a high percentage of the aldehydes on the polymer component, thereby reducing toxicity and increasing biocompatibility of the hydrogels. Typically, the time needed to cure or gel the hydrogels will vary based on a number of factors, including, but not limited to, the characteristics of the polymer component and/or dendrimer component, the concentrations of the polymer

component solution and/or the dendrimer component solution, and the characteristics of the one or more biological tissues. In embodiments, the hydrogel will cure sufficiently to provide bonding or sealing shortly after the components are combined. The gelation or cure time should provide that a mixture of the components can be delivered in fluid form to a target area before becoming too viscous or solidified and then once applied to the target area sets up rapidly thereafter. In one embodiment, the gelation or cure time is less than 120 seconds. In another embodiment, the gelation or cure time is between 3 and 60 seconds. In a particular embodiment, the gelation or cure time is between 5 and 30 seconds.

In certain embodiments, one or more foaming agents are added to the polymer component solution and/or the dendrimer component solution before the solutions are combined. In one embodiment, the foaming agents comprise a two part liquid system comprising Part 1 and Part 2, wherein Part 1 comprises a bicarbonate and Part 2 comprises an aqueous solution of di- or polyaldehydes and a titrant. A wide range of di- or polyaldhydes exist, and their usefulness is restricted largely by availability and by their solubility in water. For example, aqueous glyoxal (ethanedial) is useful, as is aqueous glutaraldehyde (pentadial). Water soluble mixtures of di- and polyaldehydes prepared by oxidative cleavage of appropriate carbohydrates with periodate, ozone or the like may also be useful.

A titrant is most preferably employed in the liquid solution of Part 2. More specifically, the titrant is an organic or inorganic acid, buffer, salt, or salt solution which is capable of reacting with the bicarbonate component of Part 1 to generate carbon dioxide and water as reaction by-products. The carbon dioxide gas that is generated creates a foam-like structure of the hydrogel and also causes the volume of the hydrogel to expand.

Most preferably, the titrant is an inorganic or organic acid that is present in an amount to impart an acidic pH to the resulting mixture of the Part 1 and Part 2 components. Preferred acids that may be employed in the practice of the present invention include phosphoric acid, sulfuric acid, hydrochloric acid, acetic acid, and citric acid.

EXAMPLES

The present invention is further illustrated by the following examples, which are not to be construed in any way as imposing limitations upon the scope thereof. On the contrary, it is to be clearly understood that resort may be had to various other aspects, embodiments, modifications, and equivalents thereof which, after reading the description herein, may suggest themselves to

one of ordinary skill in the art without departing from the spirit of the present invention or the scope of the appended claims. Thus, other aspects of this invention will be apparent to those skilled in the art from consideration of the specification and practice of the invention disclosed herein.

Unless otherwise noted, differences between groups in the following examples were examined using a two-tailed Student's *t*-test, two-way analysis of variance (ANOVA) or Log-Rank Mantel–Cox test through SPSS statistical package (version 23, SPSS Inc.). All error bars are mean ± SD of at least 3 independent experiments. Statistically significant P values were indicated in figures and/or legends as ***, $P < 0.005$; **, $P < 0.01$; *, $P < 0.05$. All *in vivo* experiments used 5 mice per treatment group. No randomization or blind events were used in animal studies.

Example 1 – *Preparation of a self-assembled RNA triple helix*

A dual-color RNA triple helix was constructed using three pieces of RNA oligonucleotides (Biosearch Technologies Inc.), denoted as miR-205 sense, miR-205 antisense, and antagomiR-221. The RNA oligomer sequences of this example are depicted in the following table:

Table 1 – RNA oligomers sequences used in the RNA triple helix assembly of Example 1

RNA oligomers	Sequences
BHQ2-5'- miR-205 sense -3'-**Cholesterol**	5' d **BHQ2**-rA-rC-rC-rA-rG-rA-rU-rU-rU-rC-rA-rG-rU-rG-rG-rA-rG-rU-rG-rA-rA-rG-rU-rUrC-rA-rG-rG-**Cholesterol** 3'
5'- miR-205 antisense -3'-**Quasar705**	5' d rC-rU-rU-rG-rU-rC-rC-rU-rU-rC-rA-rU-rU-rC-rC-rA-rC-rC-rG-rG-rA-rG-rU-rC-rU-rG- rU-rC-**Quasar 705** 3'
5'- miR-221 antagomiR -3'-**Quasar570**	5' d rC-rC-rU-rG-rA-rA-rA-rU-rC-rU-rA-rC-rA-rU-rU-rG-rU-rA-rU-rG-rC-rC-rA-rG-rG-rU-rUrG-rG-rU-**Quasar 570** 3'
BHQ2-5'- scrambled miR sense -3'-**Cholesterol**	5' d **BHQ2**-rG-rC-rA-rU-rC-rA-rA-rU-rU-rC-rU-rC-rC-rG-rA-rA-rC-rG-rU-rG-rU-rC-rA-rC-rG-rU-rU-rU-**Cholesterol** 3'
5'- scrambled miR antisense -3'-**Quasar705**	5' d rA-rC-rG-rU-rG-rA-rC-rA-rC-rG-rU-rU-rC-rG-rG-rA-rG-rA-rA-rU-rU-rG-rA-rU-rG-rC-rU-rU-**Quasar 705** 3'
5'- scrambled RNA -3'-**Quasar570**	5' d rC-rG-rA-rA-rA-rU-rA-rU-rG-rU-rC-rA-rC-rG-rG-rU-rC-rG-rC-rG-rA-rU-rC-rG-rG-rG-rA-rU-rG-rC-**Quasar 570** 3'

The miR-205 sense of this example was a 28 nucleotide (nt) RNA oligo double-modified with a Black-Hole dark quencher (BHQ2) at 5' and a cholesterol molecule at 3'.

The miR-205 antisense was a 28 nt RNA oligo modified with a near infrared (NIR) dye, QUASAR® 705 (LGC Biosearch Technologies, USA), at 3'.

The antagomiR-221 was a 30 nt RNA oligo modified with a QUASAR® 570 at 3'.

Scrambled miRs (Biosearch Technologies, USA) synthesized with the same modifications and dyes were used to form a control triple helix.

The three RNA strands were mixed in an equal molar ratio (1:1:1, final concentration 1 μM each) or several combination ratios at room temperature in an incubation buffer including 10 mM Tris buffer pH 7 (Bio-Rad) supplemented with 10 mM $MgCl_2$ (Sigma), 1 mM spermine (Sigma), and 0.8 mM of $CuSO_4$ (Sigma), and then heated to 80 °C for 5 minutes before being rapidly cooled to 4 °C.

In order to verify the RNA triple-helix formation and determine an optimal molar ratio between the three oligos of this example, fluorescence intensity of the RNA oligos (two doubles or triple helix forming structures) with graded molar ratios was measured at room temperature using a live imaging system. A nearly 100% quenching effect (no fluorescence emission) induced by the proximity of the chromophores with the quencher BHQ2 was observed at a 1:1:1 molar ratio or higher.

The emission spectra of QUASAR® 705 and 570 oligos were collected after incubation with different ratios of the oligo containing the quencher BHQ2. The fluorescence intensity of the RNA oligos at several molar ratios measured at room temperature was evaluated in order to compare quenching efficiencies, which were induced by the proximity of the chromophores with the quencher BHQ2. The region of interest (ROI) quantification of the Q570 and Q705 channels also was evaluated for several molar ratios of the components, and in the presence and absence of the quencher BHQ2.

Quenching/Fluorescence assays: The RNA strands were mixed in an equal molar ratio (1:1:1, final concentration 1 μM each) or at several combination ratios at room temperature in an incubation buffer and then heated to 80 °C for 5 minutes and rapidly cooled to 4°C. Fluorescence spectra were then taken using a microplate reader (Varioskan Flash Multimode Reader, Thermo Scientific) and fluorescence images using the IVIS Spectrum-bioluminescent and fluorescent imaging system (Xenogen XPM-2 Corporation). The Quasar570 has an Exc/Emi at 548/570 nm and the Quasar705 at 690/705 nm.

Successful self-assembly of an RNA triple helix was also confirmed using gel electrophoresis at 25 °C, which revealed slower migration rates for the RNA triple helix compared with two double-helices (including two of the three components of the RNA triple helix) and with the single RNA oligos of each component of the RNA triple helix.

The absorbance spectra of RNA oligos alone and conjugated to form the double and triple helices were collected. The triplex design afforded quenching effects between the dye/quencher pair indicating the specific spatial proximity of the three RNA oligonucleotides composing the 3D structure, and consequently, the formation of the triple-helix assembly.

These data revealed that efficient formation of the triple helix composed of the three oligos of this example (miR-205 sense and antisense and antagomiR-221) occurred at a 1:1:1 molar ratio at room temperature in the incubation buffer containing 10 mM Tris buffer (pH 7) supplemented with 10 mM $MgCl_2$, 1 mM spermine and 0.8 mM of $CuSO_4$.

Example 2 – *Characterization and competition and specificity assays*

The self-assembled RNA triple helix of Example 1 was subjected to the following characterization and competition and specificity assays.

To ensure proper triplex function *in vivo*, triplex stability was examined under (pre)clinically relevant conditions, including temperature, pH, and in the presence of urea that is capable of denaturing and dissociating dsRNAs. Extensive characterization of the triplex formation was performed using several competition assays, such as ionic strength (*see*, *e.g.*, Chiou, C.C., et al. *Analytical Biochemistry* **416**, 1-7 (2011), and Wan, C.H., et al. *J. Am. Soc. Mass. Spectr.* 20, 1281-1286 (2009)), temperature profiles, urea stability (Carlson, R.D., et al. *Biochemistry-Us* **14**, 3122-3125 (1975)), serum stability, and pH. These results corroborated the high stability of the triplex in the presence of ultra-low concentrations of magnesium, at high temperatures (*i.e.* 65°C), in physiological and super-physiological concentrations of urea, in long exposure to 50% serum, and at a pH range of 5 to 9.

Ionic strength: In the ionic strength test, the effect of Mg^{2+} and Na^{+} on the formation of the RNA triple helix on TBE gel was measured. It was revealed that Na+ decreased the probability of triple helix formation, and likely caused the formation of undesirable dimers and tetramers. **FIG. 2** depicts the effect of Mg^{2+} and Na^{+} on the formation of the RNA triple helix on TBE gel. Increasing amounts of NaCl and $MgCl_2$ were incubated with 1 μM of the RNA triple-

helix. Na^+ decreased the probability of triple helix formation and resulted in undesirable dimers and tetramers.

Presence of urea: The effect of urea concentration on the stability of the double- and triple helices were evaluated in the absence of urea, under physiological concentration (0.007 M), and at super-physiological urea concentration (7 M). Normal human adult blood typically contains between 0.004 and 0.0071 M urea, and the triple helix structures remained stable, without significant dissociation, under physiological urea concentration, and with declined dissociation in super-physiological conditions.

The concentration of single RNA and the RNA triple-helix oligos (equal molar ratio 1:1:1, final concentration 1μM each) was fixed and the samples were loaded on 20% TBE PAGE gel without and with urea (0.007 and 7M) (Invitrogen).

Different temperatures and melting experiments: The melting temperature (Tm) of the RNA oligos was examined in the triplex form (Tm=74.5 ± 3.2°C), the ssRNA oligos alone (Tm=55.1 ± 1.9°C), and the double-helix form: miR-205 sense and antisense (Tm=63.1 °C), and miR-205 sense and antagomiR-221 (Tm=64.8 ± 2.6°C). The shift in Tm of the triplex to 75°C indicated a highly stable structure.

The effect of temperature on the stability of the triple helix was evaluated by gel electrophoresis.

In the table at **FIG. 6A**, "+" indicates the presence of the specific RNA strand in the several combination samples of **FIG. 6B**, **FIG. 6C**, and **FIG. 6D**. The temperature effect on the stability of the different RNA oligo combinations evaluated by 20 % TBE gel at 25 °C, 37 °C, and 65 °C is shown at **FIG. 6B**, **FIG. 6C**, and **FIG. 6D**, respectively.

A fixed concentration of the different combinations of the RNA oligos (1 μM) was incubated at 25 °C, 37 °C, and 65 °C. At room temperature of 25 °C and at 37 °C, the stability of the triple-helix and the double-helices were identical, as shown at **FIG. 6B** and **FIG. 6C**. At 65 °C (close to the Tm of the double-helix formed between miR-205 sense as well as antisense and between miR-205 sense and antagomiR-221), dissociation of the double-helix occurred with no changes in stability for the triple-helix structure. These results were consistent with the melting temperature profiles explained in this example, which corroborated the high stability of the triplex.

The 3 RNA strands were mixed in an equal molar ratio (1:1:1, final concentration 1μM each) and were incubated for 30 minutes at 25, 37 and 65 °C and then loaded onto a 20% TBE gel (Invitrogen).

Melting experiments were conducted by monitoring the fluorescence of the SYBR® Gold (Invitrogen, USA) intercalated-RNAs using the Light Cycler 480 II Real-time PCR machine (Roche). Briefly, 1× SYBR® Gold dye (Exc/Emi = 495/537 nm, Invitrogen, USA), which was 25-100 times more sensitive than ethidium bromide and detected dsRNA, ssRNA and DNA. The single RNA and the RNA triple-helix oligos (equal molar ratio 1:1:1, final concentration 1μM each) were mixed at room temperature in incubation buffer. The RNA samples were slowly cooled from 95 to 20 °C at a rate of $0.11°C.s^{-1}$. The data were analyzed with Light Cycler 480 II Real-time PCR machine software using the first derivative of the melting profile. The first derivative of the melting temperatures was calculated as follows:

$$\frac{dRFU}{dT},$$

being the *RFU* the relative fluorescence units (from the SYBR® Gold) and the *T* the temperature (in Celsius) for each cycle of measurement. The first derivative of this function revealed whether the temperature was increasing or decreasing, and by how much it was increasing or decreasing.

In other words, for each temperature point, the average value of a reference curve was calculated and subsequently subtracted from each sample's normalized *RFU* value to generate a difference plot. Consequently, a vertical shift in fluorescence intensity on the y-axis, following reference signal subtraction, was used to identify temperature profile differences. The T_m value depicted the mean and standard deviation of three independent experiments.

Different pHs: The concentration of single RNA and the RNA triple helix oligos at a particular molar ratio (1:1:1, final concentration 1μM each) was fixed and the samples were incubated with different pH solutions (from 3 to 12) for 30 minutes and then loaded on 20% TBE gel (Invitrogen). The triple helix had remarkable stability over a pH range of 5 to 9, which corroborated the pH-independent binding of the triplex, as purine motifs of triplex were believed to present significant stability under physiological pH. The effect of pH (3 to 12) on RNA triple helix and control helix (scrambled miRs) structure was measured by gel electrophoresis, and on the emission of QUASAR® 705 and 570 on the oligos that formed the RNA triple helix. With the specific structural arrangement, the presence of quenching effects between the dye/quencher pair was believed to indicate the specific spatial proximity of the three RNA oligonucleotides

composing the 3D structure, and, consequently, the formation of the triple-helix assembly. All experiments were done in triplicate.

Stability assay in serum: Serum stability of the RNA triple helix structure and single RNA oligos were measured by gel electrophoresis after incubation in 50 % serum solution for a pre-determined period of time, and on the emission of Quasar 705 and 570 on the oligos that formed the RNA triple helix and control triplex. The single RNA and the RNA triple helix oligos were incubated in 50% fetal bovine serum (Gibco). A sample of RNA was taken at 0, 5, 10, 24, 48 and 72 hr time points after incubation at 37 °C, followed by analysis using 20% TBE gel (Invitrogen).All of these experiments were done in triplicate.

The triple helix structure was mostly intact (even after 72 hours of incubation) when compared to the single RNA oligos, which were rapidly degraded after 24 hours.

Specificity assay with recombinant Dicer and Ago2: To ensure triplex *in vivo* recognition by the transcriptional machinery following miR strands intracellular delivery, triplexes were incubated with recombinant human Dicer and AGO2/EIF2C2 enzymes. These enzymes are believed to be responsible for the recognition and unwinding by RISC and by the Argonaute protein family (specially, AGO2). The RNA triple-helix oligos were recognized and cleaved into smaller RNA products only in the presence of recombinant AGO2, when compared to the RNA triple-helices without AGO2 treatment. Therefore, the strong RNA triple-helix recognition by AGO2 depicted the self-assembled RNA triple helix as a highly specific structure.

In other words, the fluorescence signal of the dyes present in the triple helix (Q570 and Q705) was activated only at high AGO2 concentrations. AGO2 was the only enzyme able to recognized and cleave the ~20-30 nt RNA oligos (only dsRNAs larger than 300 nt), as confirmed by the absence of RNA cleaved products, and by the absence of fluorescence signal from the triple helix dyes. These results confirmed the key role of AGO2 in the recognition of the RNA triple helix.

For the recognition of miRs and the concomitant dissemble of the RNA triple-helix by the Dicer and Ago2 proteins, the RNA triple-helix was previously incubated in equal molar ratio 1:1:1, final concentration 1μM each oligo to form the structure. For DICER specificity assay, increasing amounts of recombinant human Dicer (Genlantis) from 0.5 to 2 units were incubated with 1 μM of the triple-helix oligos during 16 hours at 37ºC and then collected and inhibited by adding Dicer stop solution (Genlantis). The samples were then run on a 20% TBE gel

(Invitrogen) to evaluate the by-products of the reaction. For Ago2 assay, increasing amounts of recombinant human AGO2/EIF2C2 (Sino Biological Inc.) from 5 to 160 ng were incubated with 1 μM of the triple-helix oligos during 60 minutes at 37 °C. Reactions were stopped by incubation at 65 °C for 30 minutes. The samples were then run on a 20% TBE gel (Invitrogen) to evaluate the by-products of the reaction.

General characterization of the self-assembled RNA triple-helix was performed by Dynamic Light Scattering – DLS (Wyatt Dyna Pro Plate Reader), Zeta-Potential (Zetasizer Nano-ZS90 Malvern), Fluorescence and UV/Vis Spectroscopy and High-resolution SEM (Zeiss Merlin High-resolution SEM, EHT=3.00 kV, I Probe=80 pA, Signal A=InLens or HE-SE2) and High-resolution Cryo-TEM (JEOL 2100 FEG TEM).

Example 3 – *Formation of RNA triple helix nanoconjugates/scaffolds*

RNA triplex nanoparticles were formed by complexation of the triple helix strands of Example 1 with polyamidoamine (PAMAM) G5 dendrimer creating a branched sponge-like nanoscopic structure readily visible using cryo-electron microscopy (cryo-EM, **FIG. 1C)** and in the high-resolution scanning electron microscope (SEM, **FIG. 4, FIG. 3, FIG. 5A, FIG. 5B, FIG. 5C**) images.

Micron level RNA aggregates (3.4±1.1 μm as measured by SEM, **FIG. 4**) were formed by interactions between the RNA triplex nanoparticles (56.6±3.9 nm as measured by SEM, **FIG. 3**) and the naked PAMAM G5 dendrimer (5.3±0.7 nm as measured by cryo-EM). These nanoparticles exhibited a densely packed molecular structure approximately 50 nm in diameter, which was also confirmed by Dynamic Light Scattering (DLS) analysis, which revealed a hydrodynamic diameter of 48.4±5.7 nm. Also confirmed was the fact that the branched sponge-like dendritic structures contained complexed RNA. This test was performed with SYBR green II staining, a sensitive dye used to detect RNA. Green fluorescence emitted from the RNA triplex nanoparticles confirmed that this structure was composed of dendrimer containing RNA.

This 3D RNA structure was then allowed to react with dextran aldehyde to form a dextran-dendrimer-RNA triplex hydrogel (**FIG. 5A, FIG. 5B, FIG. 5C**) affording local administration of both the carrier and cargo while forming a strong adhesion to a tissue, such as a tumor tissue. High-resolution SEM images of the hydrogels confirmed that the triplex nanoparticles were maintained and dispersed throughout the scaffold following adhesive formation (**FIG. 5A, FIG. 5B, FIG. 5C**).

Therefore, this self-assembled platform provided control over multiple length scales: RNA triplex assembly at the nanoscale (small dendrimer triplex nanoparticles, ~50-60 nm, **FIG. 3**), dendrimer-triplex complexation followed by their aggregation at the microscale (~3-4 μm, **FIG. 4**), and adhesive hydrogel formation following dextran addition at the macroscale (>1 mm, **FIG. 5A, FIG. 5B, FIG. 5C**).

To verify dendrimer:triplex complex formation, an electrophoretic mobility shift assay (EMSA) was performed on agarose gel using increasing concentrations of PAMAM G5 (0.01 to 5 mg/mL), pre-incubated with 1 μM of the RNA triple-helix. Substantial change in the electrophoretic mobility of RNA triple-helix complexed with PAMAM G5 was evident for dendrimer concentrations higher than 0.025 mg/mL, indicating successful complexation. While PAMAM G5 alone imparted cytotoxicity in a dose dependent manner (0.1 to 5 mg/mL), its complex with RNA triplex or control triplex was cyto-compatible even at high dendrimer concentrations.

It was believed that efficacious delivery of the RNA triple-helix hydrogel nanoconjugates would be achieved by coating the breast tumor with the adhesive hydrogel scaffold that has been shown to enhance the stability of embedded nanoparticles used for local gene delivery (Conde, J. et al. *Proceedings of the National Academy of Sciences of the United States of America* **112**, E1278-E1287 (2015); and Segovia, N., et al. *Adv.Healthc.Mater.* **4**, 271-280 (2015)). A fluorescent image of the dual color RNA triple-helix in the form of a hydrogel scaffold was collected. Epi-fluorescence images following hydrogel cryo-sectioning showed a distinct and punctuate signal from the RNA triple-helix nanoparticles throughout the hydrogel network. The RNA triple helix hydrogel nanoconjugates that were pre-incubated with the complementary target for both strands show a positive fluorescent signal, whereas the ones without target did not show any fluorescent signal from the triple helix. This confirmed that individual RNA triple-helix modules complexed with the hydrogel network retained their original folding. Triple helix nanoparticles (1μM of RNA oligos complexed with 5% PAMAM G5 dendrimer) were mixed with 5% dextran aldehyde to form a hydrogel to a total of 12.5% dendrimer amine. RNA triple-helix hydrogel scaffolds showed high triplex stability with a complete discharge release within 24 to 48 hours.

RNA triple-helix hydrogel scaffold fluorescence images: Pre-cured fluorescently labeled scaffolds alone (control) or doped with triple-helix nanoparticles with or without target pre-

incubation were snap-frozen in liquid nitrogen and kept at -80°C for 24 hours. Then, 12 µm-thick cryosections (Cryostat Leica CM1850) were analyzed by fluorescence microscopy (NIS-Elements NIKON®). Controls for this experiment included empty scaffold (without nanoparticles) and scaffold with non-hybridized triple-helices (quenched fluorescence from the oligos).

RNA triple-helix release from hydrogel scaffold *in vitro*: Pre-cured disks of fluorescently labeled hydrogel scaffold alone or doped with triple-helix nanoparticles with or without target pre-hybridization were incubated in phosphate buffer saline (PBS) at 37°C. At different time points, samples were collected from the PBS and fluorescence of released products was quantified (Varioskan Flash Multimode Reader, Thermo Scientific). Data was plotted as percent of total hybridized oligo or dextran aldehyde released for each time point. Controls for this experiment included empty scaffold (without nanoparticles) and scaffold with non-hybridized triple-helices (quenched fluorescence from the oligos).

Example 4 – *In vitro RNA triple helix dendrimer nanoconjugates delivery*

The cellular uptake of a complex PAMAM G5 dendrimer (Mr. 28 kDa) with the RNA oligos was analyzed using the MDA-MB-231 TNBC cell line. To track the intracellular co-localization of PAMAM dendrimer alone and the RNA triple-helix dendrimer nanoconjugates within lysosomes the LYSOTRACKER® Blue was used to label these structures. Briefly, cells were seeded at a density of 2×10^5 cells/well in 24-well plates and grown for 24 hours prior to incubation of RNA dendrimer nanoconjugates (0.05 mg/mL of dendrimer complexed with 1 µM of triplex oligos). During the final 30 min of the incubations with the RNA dendrimer nanoconjugates, the lysosomal dye LYSOTRACKER® Blue DND-22 (Invitrogen) was included at a final concentration of 500 nM. Then, cells were fixed with 4% paraformaldehyde in 1× PBS for 15 min at 37 °C. Finally, cells were mounted in PROLONG® Gold Antifade Reagent (Invitrogen). Images of cells were taken with a NIKON®A1R Ultra-Fast Spectral Scanning Confocal Microscope.

MDA-MB-231 triple negative breast cancer cells (ATCC® Cat. No. HTB-26™, tested for mycoplasma contamination by the Division of Comparative Medicine Diagnostic Lab at MIT via IMPACT PCR, which was negative) were grown in Dulbecco's modified Eagle's medium (DMEM, Invitrogen) supplemented with 4 mM glutamine, 10 % heat inactivated fetal bovine

serum (Gibco, Life Technologies), 100 U/ml penicillin and 100 μg/ml streptomycin (Invitrogen) and maintained at 37 ºC in 5% CO2.

It was believed that nanoparticles utilize different endocytosis mechanisms for cellular uptake. Generally, endocytosis can be divided into macropinocytosis, clathrin-dependent endocytosis and caveolae-mediated endocytosis (Conner, S.D. et al. *Nature* **422**, 37-44 (2003)). To decipher the uptake mechanism of the triplex-dendrimer compared to naked dendrimer, molecules capable of inhibiting each of these cellular pathways at a time were utilized. The endocytosis inhibitors used were chlorpromazine, filipin, rottlerin, brefeldin A, colchicine and chloroquine.

In order to evaluate the uptake mechanism of the RNA triple-helix dendrimer nanoconjugates cells were treated with several internalization inhibitors. Briefly, cells were seeded at a density of 2×10^5 cells/well in 24-well plates and grown for 24 hours prior to incubation of inhibitors and RNA dendrimer nanoconjugates. Cells were then treated with chlorpromazine (10 μg/ml), or filipin (5 μg/ml), or rottlerin (10 μM), or brefeldin A (5 μM), or colchicine (10 μM) or chloroquine (10 μM) (all from Sigma) in normal culture medium for 60 min at 37 ºC. Subsequently, PAMAM dendrimer alone (0.05 mg/mL) and RNA triple-helix dendrimer nanoconjugates (0.05 mg/mL of dendrimer complexed with 1 μM of triplex oligos) were added and incubation was continued for 3 hours. Subsequently, images of cells were taken with a NIKON® A1R Ultra-Fast Spectral Scanning Confocal Microscope and the cells were analyzed by FACS.

In the absence of small-molecule inhibitors, the naked PAMAM dendrimer (labelled with ALEXA-FLUOR® 594) and the dendrimer complexed with triplex oligos (0.05 mg/mL of dendrimer complexed with 1 μM of oligos), co-localization within the lysosomes at 0, 3, 6, 24 and 48h after exposure was studied. The co-localization of naked dendrimer with the lysosomes was more evident than the dendrimer complexed with triplex oligos and decreased with time, which was consistent with the accumulation of PAMAM dendrimer in lysosomes and with the dendrimers' capability to escape the endosome via the "proton-sponge effect".

Here the "proton-sponge effect" was believed to occur when unprotonated dendrimers could absorb protons as they were pumped into the lysosome, which resulted in more protons being pumped in, leading to an increased influx of Cl^- ions and water, resulting in swelling and rupture of the lysosomal membrane with subsequent release into the cytoplasm. At 48h, the

naked dendrimer was almost completely recycled, i.e. trafficking to the extracellular milieu as the fluorescence signal decreased dramatically. However, when the dendrimer was complexed with the RNA triple-helix the co-localization of these particles with the lysosomes was no longer evident even after 48h of incubation. It was believed that these nanoconjugates did not strongly co-localize with lysosomes like the naked dendrimers, which was believed to suggest that they might enter cells via a different uptake mechanism.

In the presence of small-molecule inhibitors, the internalization and sub-cellular localization of naked dendrimers and triplex-dendrimer nanoparticles was visualized by confocal microscopy and quantified by analytical flow cytometry. A significant reduction in naked PAMAM dendrimer uptake and permeability was observed in the presence of the endocytosis inhibitors filipin (blocks caveloae endocytosis) and brefeldin A. Filipin reduced naked PAMAM uptake by 94.2 ± 2.7% and brefeldin A reduced the uptake by 92.2 ± 2.5%. These findings supported previous results that naked cationic dendrimers like PAMAM are endocytosed probably via caveloae endocytosis (Kitchens, K.M. et al. *Molecular Pharmaceutics* **5**, 364-369 (2008)).

Interestingly, when dendrimer was complexed with the RNA triple-helix oligos to form the triplex nanoparticles the uptake mechanism changed completely. A significant reduction in uptake and permeability was observed in the presence of the macropinocytosis inhibitors rottlerin and colchicine (also microtubules inhibitor). Rottlerin reduced triplex nanoparticles uptake by 78.6 ± 2.1% and colchicine reduced the uptake by 71.1 ± 1.5%. Macropinocytosis is usually initiated by extensive plasma membrane reorganization or ruffling to form an external macropinocytic structure that is then enclosed and internalized (Jones, A.T. *J Cell Mol Med* **11**, 670-684 (2007)). As macropinocytosis was dependent on microtubule function and these structures were implicated in plasma membrane ruffling, colchicine that interfered with microtubule trafficking through binding to tubulin subunits, uptake of triplex and control-triplex nanoparticles was significantly reduced. In summary, naked dendrimers and triplex dendrimers were believed to utilize completely different mechanisms to enter the cells. While naked PAMAM dendrimers utilized endocytosis to enter cells and bypass the lysosomes, the triplex dendrimer nanoconjugates were believed to utilize micropinocytosis, probably, though not wishing to be bound by any particular theory, by triggering actin-mediated membrane ruffling.

This difference in uptake mechanisms was believed to be dependent on the particles' physicochemical characteristics. Properties such as size and charge were ascertained to influence the endocytosis of these kinds of nanomaterials. Zeta-potential of naked PAMAM dendrimer (+52.7 ± 1.5 mV) and dendrimer triplex nanoparticles (−19.6 ± 4.6 mV) revealed that naked dendrimers were highly cationic whereas when complexed with the RNA triple-helix were slightly anionic. It was believed that usually the cationic particles strongly interact with the membrane and enter cells rapidly, whereas anionic particles can enter cells by binding to the positive site of the membrane (Iversen, T.G. et al. *Nano Today* **6**, 176-185 (2011)). Moreover, the size of these nanoconjugates was also significantly altered in this example. The dendrimer-triplex assembly structures size was 48.4±5.7 nm in diameter (as measured by DLS) and their aggregation occurred at the microscale (3.4±1.1 μm as measured by SEM, **FIG. 4**) while the naked dendrimer size was only 6.7±0.4 nm in diameter as measured by DLS and 5.3±0.7 nm as measured by cryo-EM. In fact, nanoparticles larger than 1 μm were most likely to be engulfed via micropinocytosis in this example, while the size involved in caveolae mediated endocytosis was about 60-80 nm (Conner, S.D. et al. *Nature* **422**, 37-44 (2003)), all of which were consistent with the dendrimer-triplex microstructure and the naked dendrimer sizes.

With an extraordinary cellular uptake efficiency, analytical flow cytometry data showed that RNA triplex nanoparticles (0.05 mg/mL of dendrimer complexed with 1 μM of triplex oligos) were able to transfect nearly 100% (99.8 ± 2.5%) of the cancer cells with a strong and uniform signal from both dyes (Q705 and Q570) (**FIG. 7A**, **FIG. 7B**, **FIG. 7C**, **and FIG. 7D**). The RNA-dendrimer complexes accumulated in MDA-MB-231 cells as verified by confocal microscopy at 24 h. Confocal imaging showed efficient uptake of the RNA-dendrimer into targeted cells, as demonstrated by the outstanding co-localization and overlap of the dual color RNA triple-helix at 24 h.

Specifically, flow cytometry revealed at **FIG. 7A**, **FIG. 7B**, **FIG. 7C**, **and FIG. 7D** the specific uptake of fluorescent RNA-dendrimer nanoparticles into MDA-MB-231 cells. Negative and positive controls were cells only and cells treated with the RNA double-helices (Q705:BHQ2 and Q570:BHQ2), respectively. The confocal images indicated strong uptake of the RNA-dendrimer complexes, as demonstrated by the outstanding co-localization of the dual color RNA triple-helix (Q705:Q570:BHQ2). Nuclei (in blue) were stained with DAPI. Scale

bars, 10 μm. All experiments were done in triplicate and errors reported as standard deviation (s.d).

The flow cytometry was collected by the following procedure: MDA-MB-231 cells incubated with naked PAMAM G5 dendrimer alone or RNA oligos complexed with PAMAM G5 dendrimers were washed with PBS and detached with 0.25% trypsin-EDTA (Life Technologies). FACS running buffer (500 μl), consisting of 98% PBS and 2% heat inactivated fetal bovine serum (Gibco, Life Technologies), was added to each well. Cells were mixed thoroughly and then transferred to FACS tube with filter lid, and the Alexa-Fluor 594 (for naked dendrimer) and Q705 and Q570 (for triplex) signals were acquired on FACS LSR Fortessa HTS-1 (BD Biosciences) flow cytometer.

Confocal images of cellular uptake kinetics for cells incubated with RNA triplex nanoparticles for 0.5, 3, 6, 24, and 48 h were taken, and indicated that the triplex nanoparticles were internalized by cells at 3h with a maximum peak of cellular uptake at 48h. A quantification of fluorescence from punctuated structures using Image-J software (version 1.48) was also collected. These experiments were done in triplicate and the error bars were plotted as standard deviation. The evaluation of cellular uptake was also performed following the administration of both RNA double-helices separately. However, flow cytometry and confocal data revealed only moderate uptake efficiency of 38% (38.3 ± 7.6%) for each of the RNA double-helices when provided separately, when compared to the excellent uptake of the triple-helix (99.8 ± 2.5%), confirming that co-transfection with RNA triple-helix was far more efficacious. Higher triplex efficacy was believed to be a result, at least in part, of improved triplex stability. Additionally, the dendrimer amine binding groups available for interaction with the double or triple helices were finite, hence higher 'effective' amount of each sequence were complexed to the dendrimer surface when in a triplex structure.

Example 5 – *Impact of miRs delivery on breast cancer cells' phenotype*

The impact of miRs delivery on cancer cells was evaluated. First confirmed was the reduction in miR-221 (oncogenic) expression level and enhancement of miR-205 expression (tumor suppressor) following treatment with the RNA triple-helix compared with the control triple-helix (triplex formed with scrambled miR sequences) after 24, 48 and 72h of incubation (**FIG. 8**). **FIG. 8** depicts miR-205 and miR-221 expression in breast cancer cells at 24, 48, and 72 hours of incubation (n = 3, statistical analysis performed with a two-tailed Student's t-test, **,

$P < 0.01$; miRNA levels were normalized to *RNU6B* reference gene). To corroborate these results, a luciferase reporter was constructed to assess RNA triplex nanoparticles activity, which proved the functional role of altering the expression of the studied miRNAs in abrogating cancer.

For dual luciferase reporter experiments, the miRNA sensor was generated by inserting the antisense sequence to miR-205 or the sense sequence to miR-221 into the 3' untranslated region of Luciferase on vector. These cloning vectors were produced by Cyagen Biosciences Inc. The vectors were constructed in *E. coli Stbl3* host to ensure sequence stability with ampicillin as the antibiotic resistance marker. The *E.coli* transformed with the vectors were grown in Luria-Bertani (LB) broth (Invitrogen) supplemented with 100 μg/mL of ampicillin (Invitrogen) at 37°C overnight. After this, the vectors were extracted and purified from the cultured *E. coli* using a Plasmid Midi Kit (Qiagen). For vector transfection in human breast cancer cells, MDA-MB-231 cells not expressing luciferase were stably transfected with miR-Luc-vectors (1 μg per well) using LIPOFECTAMINE® 3000 (Invitrogen) according to the manufacturer's protocol. Cell lysates were measured with 150 μg/mL of D-luciferin (Caliper LifeSciences) for luciferase activity after 48 hours of luciferase vectors transfection. Then cells were incubated with increasing amounts of the RNA triple-helix dendrimer nanoconjugates and controls for 24, 48 and 72 hours and the optimal sensor activity was evaluated by fluorescent imaging system (Xenogen XPM-2 Corporation) and quantification of cell lysates luminescence using a microplate reader (Varioskan Flash Multimode Reader, Thermo Scientific).

Then examined were the phenotypic effects of miR replacement and oncomiR inhibition via RNA triple-helix vehicle in tissue culture. Hence, the tumorigenicity of MDA-MB-231 cells was evaluated by measuring the IC_{50} via an MTT assay (**FIG. 9**), cell migration/proliferation via a wound closure assay (**FIG. 10**) and cell growth and viability using a clonogenic survival assay with crystal violet (**FIG. 11**) following treatment with RNA-dendrimer complexes (0.05 mg/mL of dendrimer complexed with 1 μM of triplex oligos). RNA triple-helices significantly inhibited the growth of MDA-MB-231 cells compared with the two double-helices (Q570 and Q705), and with a control triplex (**FIG. 9**).

FIG. 9 depicts cell viability via an MTT assay for 24, 48 and 72 hours (n=3, statistical analysis performed with a two-tailed Student's *t*-test, **, $P < 0.01$; *, $P < 0.05$). As shown at **FIG. 10**, RNA triple-helix nanoparticles restricted MDA-MB-231 cell migration. As shown at **FIG. 11**, the number of colonies in the cells transfected with the RNA triple-helix was compared

with control triplex at 24, 48 and 72 hours of incubation. **FIG. 11** depicts the absorbance of the crystal violet stained colonies (dissolved in methanol) at 540 nm (n=3, statistical analysis performed with a two-tailed Student's *t*-test, **, $P < 0.01$; *, $P < 0.05$). All experiments were done in triplicate and error bars plotted as standard deviation (s.d).

Cell migration and proliferation was studied using a wound closure assay where cells were allowed to grow in a 24-well plate until confluency and a wound was created using a sterile pipet tip. The cells were then incubated with the RNA-dendrimer complexes and wound closure was monitored using light microscopy. Cells treated with a control triplex were able to close the wound almost completely (~90%) within 72 h (**FIG. 10**). Cells treated with the two double-helix miRs separately showed a partial closure of the wound over this time frame (75% for Q570 and 35% for Q705 oligos), while cells treated with the RNA triple-helix were not able to close the wound at all. These data indicated that the delivery of both mimic miR-205 and antagomiR-221 almost completely eliminated the motility of MDA-MB-231 cells (**FIG. 10**). A remarkable reduction in cell survival of about 95% following RNA triple-helix delivery was observed after 72 hours of incubation using a clonogenic survival assay, when compared with a control triplex (**FIG. 4D**, **FIG. 11**).

Taken together, these data were believed to confirm that the dual miR delivery provided by the RNA triple-helix for the replacement of the miR-205 and the inhibition of the miR-221 exploited endogenous pathways to exert the desired phenotypic response of breast cancer cells, controlling the cell migratory behavior.

Cell viability and proliferation assays: A standard MTT [3-(4,5-dimethylthiazol-2-yl)-2,5-diphenyltetrazoliumbromide] reduction assay (MOLECULAR PROBES®, Life Technologies) was performed to determine the viability of cells to increasing concentrations of PAMAM G5 dendrimer alone and complexed with RNA oligos. Cells were seeded at a density of 1×10^5 cells per well in 24-well culture plates in complete DMEM (500 µl) with serum. After 24 hours of exposure to dendrimer with and without RNA oligos, the medium was removed and the cells were washed twice with sterile PBS and 300 µl of fresh medium with serum was added. Then 16.7 µl of sterile MTT stock solution (5 mg/mL in PBS) was added to each well. After incubation for an additional 2 hours, the medium was removed and the formazan crystals were resuspended in 300 µl of dimethyl sulfoxide (Sigma). The solution was mixed and its absorbance was measured at 540 nm as a working wavelength and 630 nm as reference using a microplate

reader (Varioskan Flash Multimode Reader, Thermo Scientific). The cell viability was normalized to that of cells cultured in the culture medium with PBS treatment.

For the wound closing assay (frequently used for evaluating migration rates of cells in culture), MDA-MB-231 cells were grown to >95% confluency in a 24-well plate and a wound was made using a sterile pipet tip. The cells were then incubated with the RNA-dendrimer complexes and the wound closure was monitored using light microscopy.

In the clonogenic survival assay, at 24 hours after transfection, MDA-MB-231 cells were harvested and resuspended in the culture medium. In 24-well plates, 1×10^5 cells/well were seeded and allowed to grow until visible colonies formed (6 days). Cell colonies were fixed using 4% paraformaldehyde (Sigma) for 5 minutes at 37 ºC and stained with 0.05% crystal violet (Sigma) in Mili-Q water filtered at room temperature for 30 minutes. Cell colonies were then washed three times with water and incubated in a half of the total well volume of methanol (Sigma) to solubilize the dye. Then, the absorbance at 540 nm was measured using a microplate reader (Varioskan Flash Multimode Reader, Thermo Scientific). Each sample had three replicates and the mean ± SD.

Example 6 – *In vivo miRNA modulation via RNA triple helix scaffolds*

The *in vivo* nanoconjugates pharmacokinetics and platform therapeutic efficacy in an orthotopic breast cancer mouse model was studied. The efficacy of the gene-therapy based therapeutic platform was compared to chemotherapy drugs that are part of the current standard of care for human breast cancer including doxorubicin (DOX), paclitaxel (PTX), and the monoclonal antibody bevacizumab (AVASTIN®).

Two miR oligonucleotides forming a triple-helix were used for *in vivo* miR inhibition strategy (antagomiR, a small synthetic ssRNA used to inhibit an oncomiR) and miR replacement therapy (miR mimic, a mature miR duplex composed of both sense and antisense strands used as tumor suppressor) in an orthotopic triple-negative breast cancer (TNBC) mouse model. TNBC is characterized by lack of progesterone, estrogen and HER2 receptors. Thus, TNBC was not responsive to conventional hormonal therapy (such as tamoxifen or aromatase inhibitors) or therapies that target HER2 receptors, such as HERCEPTIN® (trastuzumab), which is a biological macromolecule for targeted therapy. Hence, TNBC could benefit from gene therapy approaches, including endogenous miR modulation. It was believed that when a miRNA that was up-regulated intimately contributed to breast cancer progression (e.g. miR-221^0), an

oncogenic miR inhibition therapy could be used to sterically hinder the miR expression via an antagomiR. Additionally, if a miR was downregulated in breast cancer (e.g. miR-205), the delivery of mature miRs (miR mimic oligonucleotide with the same sequence as the endogenous mature miR) would restore balanced miR expression levels.

Development of orthotopic triple negative breast cancer mice model: Tumors in the mammary fat pad were induced in female SCID hairless congenic mice (SHC™ Mouse CB17.Cg-Prkdc^{scid}Hr^{hr}/IcrCrl from Charles River Laboratories International, 6 weeks, n=5) by injection of 5×10^6 MDA-MB-231 cells stably expressing firefly luciferase, suspended in 50 μL of HBBS (Lonza) solution. For determination of tumor growth, individual tumors were measured using caliper and tumor volume was calculated by tumor volume (mm^3) = width × ($length^2$) / 2. Treatments began when tumor volume reached about 100 mm^3.

Hydrogel scaffolds loaded with the RNA oligos (1μM of RNA oligos doped in 5% PAMAM G5 dendrimer) or drugs (at final concentration: DOX= 0.8 μM; PTX= 300 μM; Avastin= 0.07 μM) were implanted adjacent to the tumor in the mammary fat pad of SCID hairless congenic mice when tumors reached a desired volume of ~100 mm^3. Inhibition of tumor progression was measured by luciferase expression while each RNA oligo release was tracked fluorescently via live imaging system for two weeks post-hydrogel implantation. No signs of inflammation were observed at the surgical site and no changes in body weight were observed before or after breast tumor induction or hydrogel implantation, which was believed to suggest that the hydrogels were biocompatible with no associated toxicity or side effects. Bioluminescence imaging of mice and tumor size measurements revealed that only the RNA triple-helix hydrogel scaffolds (that carried the mimic miR-205 and the antagomiR-221) were able to promote efficient and sustained inhibition of tumor progression, with almost 90% tumor size reduction ($n = 5$, $P < 0.001$) 13 days after hydrogel disk implantation. Conversely, 50% tumor reduction was attained following each miR administration separately, while hydrogel only, control triplex (scrambled miRs) and Avastin-loaded hydrogel showed no tumor size reduction. Dox and PTX-loaded hydrogels showed a 25% and 35% reduction in tumor size, respectively.

Treatment with drug-loaded hydrogels revealed that at early time points (1 to 3 days) the administration of DOX and PTX significantly reduced the onset of tumor progression (as judged by tumor size and *in vivo* luciferase signal). However, this reduction was temporary and diminished as the tumor continued to grow. Traditional chemotherapeutic agents are often

associated with recurrence of tumor after several days of treatment requiring multiple administrations, which is consistent with these results. The high efficacy following miR delivery was believed to stem from the selective and specific delivery to tumor cells only compared with the nonselective chemotherapeutic drug uptake. The strategy herein of inhibiting an oncogenic miR-221 and providing a tumor suppressor miRNA (miR-205) simultaneously caused a potent and long lasting tumor inhibition.

Non-invasive longitudinal monitoring of tumor progression was followed by scanning mice with the IVIS Spectrum-bioluminescent and fluorescent imaging system (Xenogen XPM-2 Corporation) from mice bearing mammary tumors from MDA-MB-231 cells (n=5 animals per treated group). 15 minutes before imaging, mice were intraperitoneally injected with 150 µL of D-luciferin (30 mg/mL, Perkin Elmer) in DPBS (Lonza). Whole-animal imaging was performed at the indicated time points – 0, 2, 6, 24, 48, 72 hours and days 5, 7, 9 and 13. Assessment of *in vivo* toxicity via mice body weight evaluation was performed on all the animal groups during 32 days after tumor induction and hydrogel exposure. Histological sections of the tumors (n=5) were stained with hematoxylin and eosin and for immunohistochemical analysis the tumors (n=5) were stained with the antibody anti-Ki67 (Abcam ab15580, dilution 1:200).

RNA nanoconjugates uptake and biodistribution were examined by quantifying fluorescence images of mice organs (liver, kidneys, spleen, heart, lungs and intestines) 13 days post-implantation. At 13 days, 20-30% of the miRs persisted in the tumoral tissue exclusively, when compared to major organs. No fluorescent signal was found in any of the major organs. A time curve documenting the triplex signal (Q705 and Q570 dyes) in organs harvested from mice treated with the RNA triple-helix hydrogel scaffolds for 2, 6, 24, 48, 72 h and days 5, 8, 11 and 13 was collected. The triplex nanoparticles accumulated exclusively in the tumor tissue as demonstrated by *ex vivo* images of the organs and time curves for each organ. There appeared to be no accumulation of the triplex nanoparticles in any major organ at all time points during the 13 days, except some background signal in the intestine (also observed at 0h of incubation).

Staggered release kinetics of the two miRs was observed. The maximum fluorescence peak occurred at 24 h for the tumor suppressor miR-205 and only at 48 h for the antagomiR of the miR-221. The staggered kinetics were believed to suggest that the miR-205 was initially processed by the RISC complex and by Ago2 compared to the antagomiR. Taken together, these results indicated that the system was able to initially enhance the expression of a tumor

suppressor miR, and 24 h later to inhibit the oncogenic miR responsible for breast tumor progression and proliferation. The data confirmed the capacity of this platform to provide efficient *in vivo* miR replacement therapy and to promote oncogenic miR inhibition.

H&E staining of breast tumor sections showed evidence of extensive reduction in vascularization for mice treated with RNA triple-helix scaffold, when compared to control triplex, in accordance with tumor size reduction due to miRNAs delivery to tumor microenvironment. An increasing number of large blood vessels could be found in the control triplex groups. Immunohistochemical analysis showed that the expression of Ki67, a cellular marker strictly associated with cell proliferation, was reduced only after treatment with hydrogels embedded RNA triple-helix nanoparticles.

Example 7 - *Survival study and analysis of tumor genetic expression profile*

A survival study was performed for mice treated with hydrogel scaffolds loaded with the triplex and control triplex, as well as for the chemotherapeutic drugs (DOX, PTX and Avastin). Mice implanted with RNA triple-helix hydrogel scaffolds showed a highly significant survival advantage (P=0.006) compared with hydrogel only, with control triplex hydrogels and with drug-loaded hydrogels. Survival seemed to correlate with the significant tumor size reduction observed mainly in mice treated with RNA triple-helix hydrogel scaffolds.

Following miR delivery, an investigation was performed of the tumor genetic expression profile of *LAMC1*, *E2F1* and *p53* (regulated by miR-205) and *E-cadherin*, *Snail1* and *Slug* (*Snail2*) (regulated by miR-221). These key genes are believed to be major regulators of cell cycle progression (*E2F1*), tumor suppressor (*p53*) or major components of extracellular matrix involved in cell adhesion, proliferation and migration (*LAMC1*, *E-cadherin*, *Snail1* and *Slug*). A heat map was created, which depicted qPCR analysis of RNA extracted from resected tumors. Quantitative PCR determination of gene expression levels in mice treated groups for all the studied genes was collected. This genetic screening showed that miR-205 directly targeted *LAMC1*, a protein altered in human breast cancer that has been implicated in a wide variety of biological processes including cell adhesion, differentiation, proliferation, migration, signaling, and metastasis. When miR-205 expression was enhanced by the triple-helix scaffold, the expression of *LAMC1* decreased considerably, altering cancer cells proliferation as corroborated by the foregoing *in vitro* and *in vivo* data. miR-205 also directly targeted *E2F1*, a gene that was

overexpressed in triple-negative breast tumors (Piovan, C., *et al. Mol Oncol* **6**, 458-472 (2012)), in which the level of miR-205 was low.

It was determined that increasing the miR-205 expression by the delivery of RNA triple-helix scaffolds substantially decreased the expression of *E2F1*. Hence, these results demonstrated that *E2F1* was a target of miR-205 in triple negative breast cancer tissues. Also, *p53* acted like an enhancer of miR-205 expression as the increase in the expression of this miR was followed by the up-regulation of *p53*. miR-221 expression, which was found to be up-regulated in triple-negative breast tumors and in a panoply of cancer types (Nassirpour, R. et al. *Plos One* **8**(2013)), has been shown to directly target proliferation and adhesion genes, such as *E-cadherin*, *Snail1* and *Slug* (*Snail2*).

It was determined that the inhibition of miR-221 altered *E-cadherin* expression and its regulatory transcription factors *Snail* and *Slug*, with a corresponding strong reduction in cell migration and invasion in breast tumors. Down regulation of miR-221 increased *E-cadherin* levels and decreased the expression levels of *Snail* and *Slug*. Moreover, the expression of *VEGF* was highly downregulated, in particular in mice treated with RNA triple-helix scaffolds, where the inhibition of tumor size was more significant. Taken together, it was believed that these gene expression data validated the ability of the RNA triple-helix scaffold to inhibit oncogenes and to enhance immunosuppression capacity, which resulted in efficient tumor reduction of nearly 90%, achieved only following dual miR therapy.

Quantitative PCR for miRNA expression: Total RNA from MDA-MB-231 cells and breast tumors from SCID xenografted mice was extracted using RNeasy Plus Mini Kit (Qiagen) according to the manufacture's protocol. cDNA was produced using High-Capacity cDNA Reverse Transcription Kit (Applied Biosystems) using 500 ng of total RNA. qRT-PCR was performed with Taqman miRNA assays and Taqman probes FAM-MGB for miR-205, miR-221, VEGF, LAMC1, E2F1, p53, E-cadherin, Snail1 and Slug (Snail2) (Applied Biosystems). RNU6B was used as a reference gene. The reactions were processed using Light Cycler 480 II Real-time PCR machine (Roche) using TaqMan® Gene Expression Master Mix (Applied Biosystems) under the following cycling steps: 2 min at 50 °C for UNG activation; 10 min at 95 °C; 40 cycles at 95 °C for 15 s; 60 °C for 60 s. At least three independent repeats for each experiment were carried out. Gene expression was determined as a difference in fold after normalizing to the housekeeping gene RNU6B.

RNA triple-helix hydrogel scaffold synthesis and *in vivo* implantation: Tagged hydrogel scaffolds were developed as previously described (Oliva, N., *et al. Langmuir* **28**, 15402-15409 (2012)). Briefly, equal parts of dendrimer amine of 12.5% solid content and dextran aldehyde 5% solid content with 0.25% fluorescently labeled dextran were mixed to form 6 mm pre-cured disks. For doped scaffolds, RNA nanoparticles (1μM of RNA oligos doped in 5% PAMAM dendrimer generation 5 with 100% amines) or the free drugs: doxorubicin (DOX, from LC Laboratories), paclitaxel (PTX, from LC Laboratories) and the monoclonal antibody bevacizumab (Avastin® from Roche) were added to the dendrimer solution prior to hydrogel formation. All solutions were filtered through a 0.22 μm filter prior to hydrogel formation for *in vivo* implantation. Pre-cured disks of fluorescently labeled scaffold with or without RNA nanoparticles were formed and implanted subcutaneously on top of the mammary tumor in mice.

Dextran aldehyde tagging reaction: Dextran aldehyde (Mr 10,000 Da, 50% oxidation; 10 mg) was tagged by reaction with 2 mg of Alexa-Fluor® 405 Cadaverine (Invitrogen) in 20 mL of 50 mM carbonate buffer (pH 8.5) for 1 hour at room temperature. Then, the reaction crude was cooled down in an ice-water bath and imine bonds were reduced with 20 mL of 30 mM sodium cyanoborohydrate in PBS for 4 hours. Then, tagged dextran aldehyde was dialyzed four times through a 3,000 Da MWCO Centrifugal Filter (Millipore) for 20 min each time at room temperature and 4,000 RCFs. The purified product was lyophilized.

We claim:

1. A composition comprising:

an miRNA triple helix comprising an miRNA sense oligonucleotide, an miRNA antisense oligonucleotide, and an antagomiRNA oligonucleotide,

wherein the miRNA sense oligonucleotide and the miRNA antisense oligonucleotide are associated with each other by a plurality of Watson-Crick hydrogen bonds, and

the antagomiRNA oligonucleotide and the miRNA sense oligonucleotide are associated with each other by a plurality of Hoogsteen hydrogen bonds.

2. The composition of claim 1, wherein the miRNA antisense oligonucleotide is a tumor suppressor miRNA.

3. The composition of claim 1 or 2, wherein the miRNA sense oligonucleotide is an miR-205 sense oligonucleotide, and the miRNA antisense oligonucleotide is an miR-205 antisense oligonucleotide.

4. The composition of claim 1 or 2, wherein the antagomiRNA oligonucleotide is an antagomiR-221 oligonucleotide.

5. The composition of claim 1, wherein the molar ratio of the miRNA antisense oligonucleotide to the miRNA sense oligonucleotide to the antagomiRNA oligonucleotide is about 1:1:1.

6. The composition of claim 1, further comprising a dendrimer having at least two branches with one or more surface groups, wherein the RNA triple helix is associated with the one or more surface groups of the dendrimer.

7. The composition of claim 6, wherein 100 % of the one or more surface groups comprise at least one primary or secondary amine.

8. The composition of claim 6 or 7, wherein the dendrimer is a G5 PAMAM dendrimer.

9. The composition of claim 6, wherein the composition comprising the dendrimer and the RNA triple helix associated with the dendrimer is a particulate material having an average largest dimension of about 30 nm to about 80 nm.

10. The composition of claim 9, wherein the composition comprises a plurality of aggregates of the particulate material, the aggregates having an average largest dimension of about 1 μm to about 10 μm.

11. A therapeutic composition comprising:

a hydrogel comprising

a polymer having one or more aldehyde groups, and

a first dendrimer having at least two branches with one or more surface groups, wherein at least a portion of the one or more surface groups comprise at least one primary or secondary amine; and

at least one RNA triple helix associated with a second dendrimer having at least two branches with one or more surface groups;

wherein the at least one RNA triple helix is disposed in the hydrogel, and comprises an miRNA sense oligonucleotide, an miRNA antisense oligonucleotide, and an antagomiRNA oligonucleotide,

wherein the miRNA sense oligonucleotide and the miRNA antisense oligonucleotide are associated with each other by a plurality of Watson-Crick hydrogen bonds, and

the antagomiRNA oligonucleotide and the miRNA sense oligonucleotide are associated with each other by a plurality of Hoogsteen hydrogen bonds.

12. The therapeutic composition of claim 11, wherein 100 % of the one or more surface groups of the second dendrimer comprise at least one primary or secondary amine.

13. The therapeutic composition of claim 11 or 12, wherein about 20 % to about 75 % of the one or more surface groups of the first dendrimer comprise at least one primary or secondary amine.

14. The therapeutic composition of claim 11 or 12, wherein about 25 % of the one or more surface groups of the first dendrimer comprise at least one primary or secondary amine.

15. The therapeutic composition of claim 11, wherein the at least one RNA triple helix is disposed substantially evenly in the hydrogel.

16. The therapeutic composition of claim 11, wherein the miRNA antisense oligonucleotide is a tumor suppressor miRNA.

17. The therapeutic composition of claim 11, wherein the miRNA sense oligonucleotide is an miRNA-205 sense oligonucleotide, and the miRNA antisense oligonucleotide is an miRNA-205 antisense oligonucleotide.

18. The therapeutic composition of claim 11, wherein the antagomiRNA oligonucleotide is an antagomiR-221 oligonucleotide.

19. The therapeutic composition of claim 11, wherein the molar ratio of the miRNA antisense oligonucleotide to the miRNA sense oligonucleotide to the antagomiR oligonucleotide is about 1:1:1.

20. A kit for making a therapeutic composition comprising:

a first part which includes a first solution comprising a polymer component, wherein the polymer component comprises a polymer; and

a second part which includes a second solution comprising a dendrimer component, wherein the dendrimer component comprises a first dendrimer having at least 2 branches with one or more surface groups, and a second dendrimer having a least 2 branches with one or more surface groups associated with an RNA triple helix;

wherein the RNA triple helix comprises an miRNA sense oligonucleotide, an miRNA antisense oligonucleotide, and an antagomiRNA oligonucleotide, wherein the miRNA sense oligonucleotide and the miRNA antisense oligonucleotide are associated with each other by a plurality of Watson-Crick hydrogen bonds, and the antagomiRNA oligonucleotide and the miRNA sense oligonucleotide are associated with each other by a plurality of Hoogsteen hydrogen bonds.

21. The kit of claim 20, wherein 100 % of the one or more surface groups of the second dendrimer comprise at least one primary or secondary amine.

22. The kit of claim 20 or 21, wherein about 20 % to about 75 % of the one or more surface groups of the first dendrimer comprise at least one primary or secondary amine.

23. The kit of claim 20 or 21, wherein about 25 % of the one or more surface groups of the first dendrimer comprise at least one primary or secondary amine.

24. The kit of claim 20, wherein the polymer comprises dextran substituted with three or more aldehyde groups.

25. The kit of claim 20, wherein the miRNA antisense oligonucleotide is a tumor suppressor miRNA.

26. The kit of claim 20, wherein the miRNA sense oligonucleotide is an miR-205 sense oligonucleotide, and the miRNA antisense oligonucleotide is an miR-205 antisense oligonucleotide.

27. The kit of claim 20, wherein the antagomiRNA oligonucleotide is an antagomiR-221 oligonucleotide.

28. The kit of claim 20, wherein the molar ratio of the miRNA antisense oligonucleotide to the miRNA sense oligonucleotide to the antagomiRNA oligonucleotide is about 1:1:1.

29. A method for treating a biological tissue, the method comprising:

providing a first solution comprising a polymer component, wherein the polymer component comprises a polymer having three or more aldehyde groups;

providing a second solution comprising a dendrimer component, wherein the dendrimer component comprises a first dendrimer having at least 2 branches with one or more surface groups, and a second dendrimer having a least 2 branches with one or more surface groups associated with an RNA triple helix; and

combining the first and second solutions together to produce a therapeutic composition and contacting one or more biological tissues with the therapeutic composition;

wherein the RNA triple helix comprises an miRNA sense oligonucleotide, an miRNA antisense oligonucleotide, and an antagomiRNA oligonucleotide, wherein the miRNA sense oligonucleotide and the miRNA antisense oligonucleotide are associated with each other by a plurality of Watson-Crick hydrogen bonds, and the antagomiRNA oligonucleotide and the miRNA sense oligonucleotide are associated with each other by a plurality of Hoogsteen hydrogen bonds.

30. The method of claim 29, wherein 100 % of the one or more surface groups of the second dendrimer comprise at least one primary or secondary amine.

31. The method of claim 29 or 30, wherein about 20 % to about 75 % of the one or more surface groups of the first dendrimer comprise at least one primary or secondary amine.

32. The method of claim 29 or 30, wherein about 25 % of the one or more surface groups of the first dendrimer comprise at least one primary or secondary amine.

33. The method of claim 29, wherein the polymer is dextran.

34. The method of claim 29 or 33, wherein the dendrimer is a G5 PAMAM dendrimer.

35 The method of claim 29, wherein the miRNA sense oligonucleotide is a tumor suppressor miRNA.

36. The method of claim 29, wherein the miRNA sense oligonucleotide is an miR-205 sense oligonucleotide, and the miRNA antisense oligonucleotide is an miR-205 antisense oligonucleotide.

37. The method of claim 29, wherein the antagomiRNA oligonucleotide is an antagomiR-221 oligonucleotide.

38. The method of claim 29, wherein the molar ratio of the miRNA antisense oligonucleotide to the miRNA sense oligonucleotide to the antagomiRNA oligonucleotide is about 1:1:1.

39. A method comprising:

coating a tumor *in vivo* with an adhesive hydrogel composition comprising an RNA triple helix, wherein the RNA triple helix comprises an miRNA mimic and an antagomiRNA.

40. The method of claim 39, wherein the adhesive hydrogel composition comprises a dendrimer associated with the RNA triple helix.

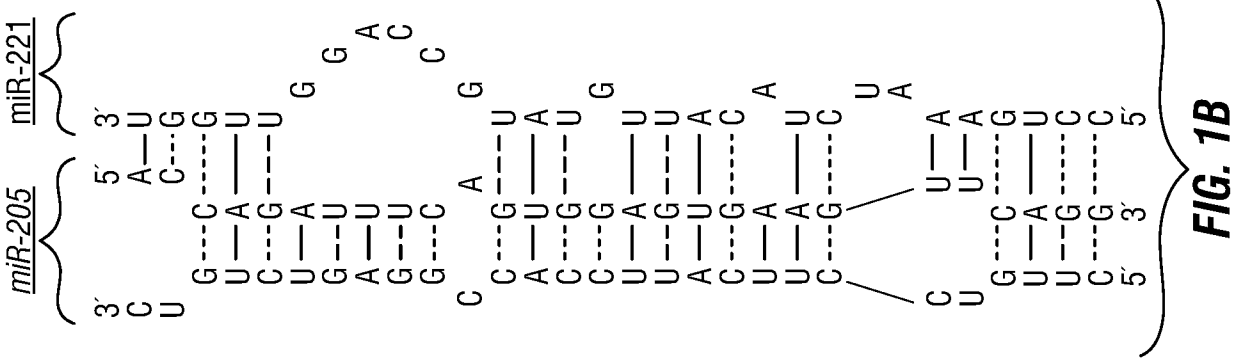
miR-205
miR-221

FIG. 1B

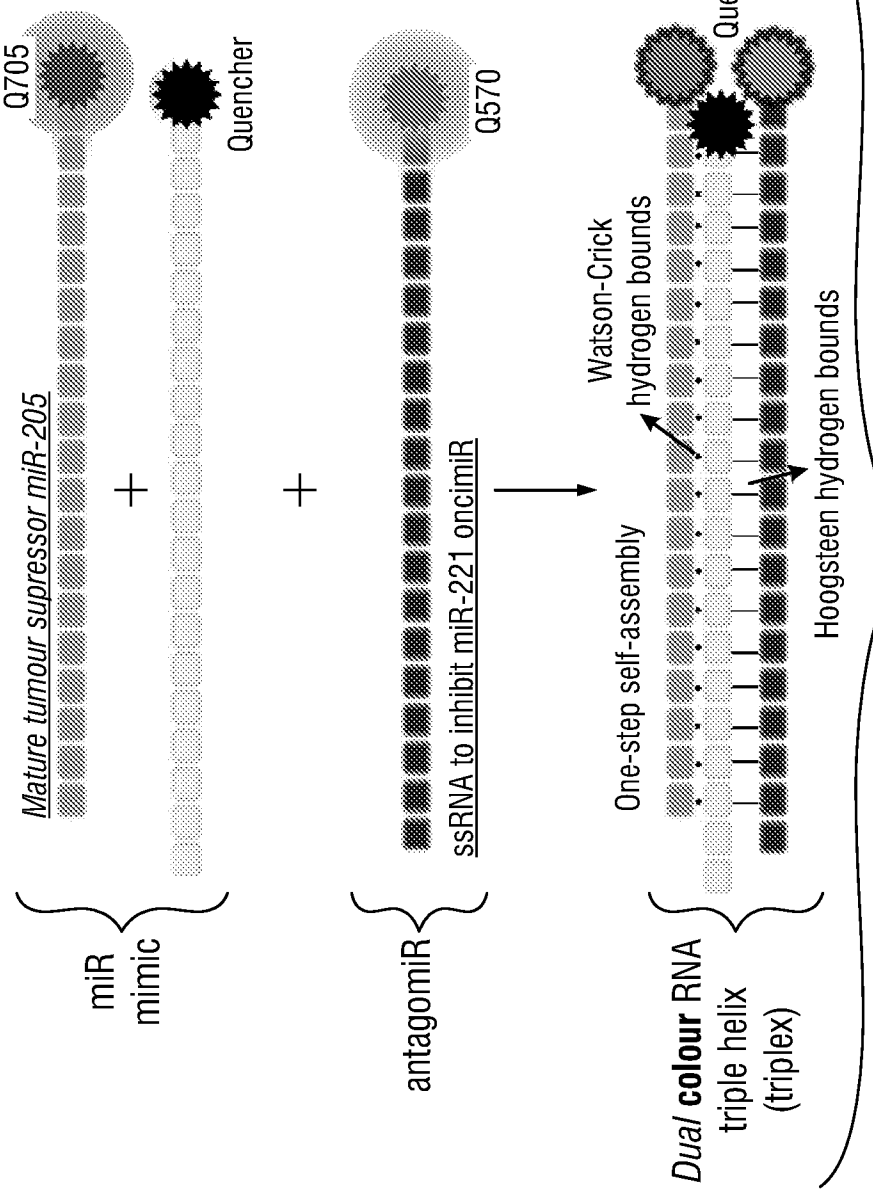
Mature tumour supressor miR-205
Q705
Quencher
miR mimic
ssRNA to inhibit miR-221 oncimiR
Q570
antagomiR
One-step self-assembly
Watson-Crick hydrogen bounds
Quenching
Hoogsteen hydrogen bounds
Dual colour RNA triple helix (triplex)

FIG. 1A

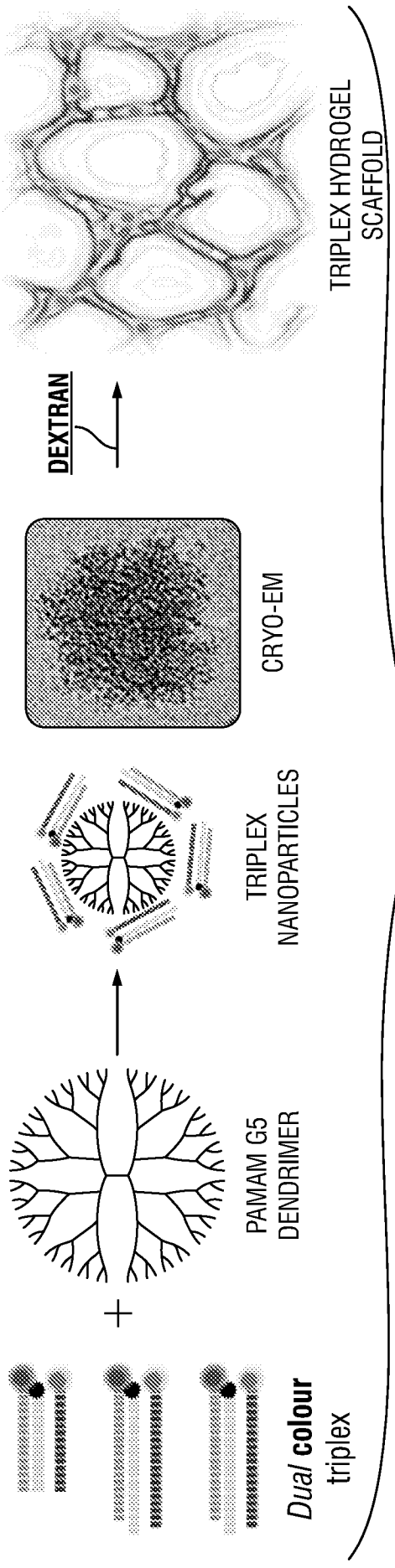
Dual colour triplex
PAMAM G5 DENDRIMER
TRIPLEX NANOPARTICLES
CRYO-EM
DEXTRAN
TRIPLEX HYDROGEL SCAFFOLD

FIG. 1C

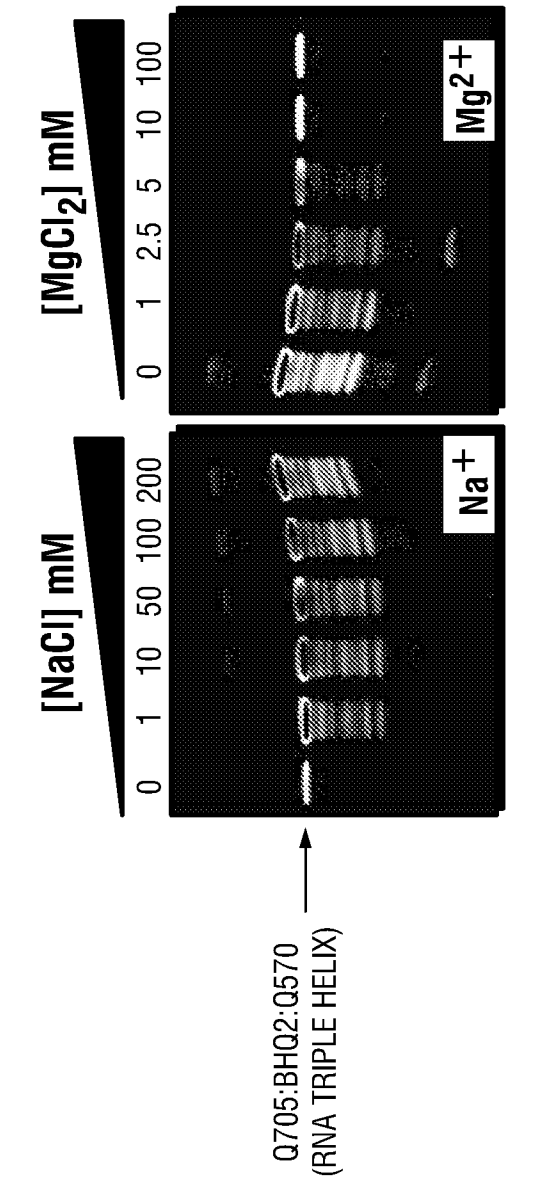
[NaCl] mM
0 1 10 50 100 200
Na+
[MgCl2] mM
0 1 2.5 5 10 100
Mg2+
Q705:BHQ2:Q570
(RNA TRIPLE HELIX)

FIG. 2

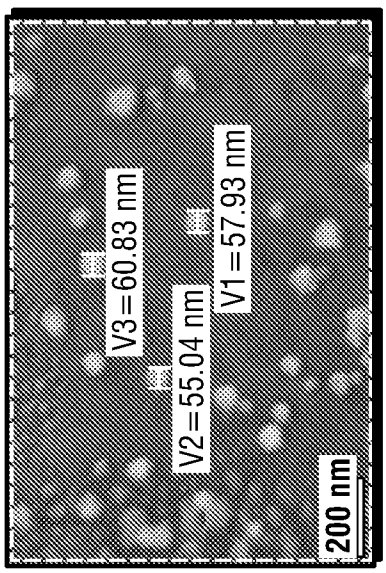

FIG. 3

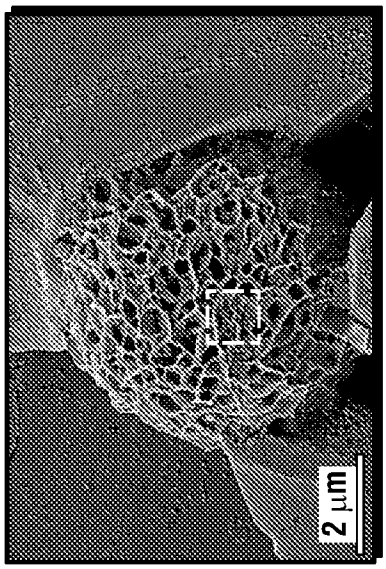

FIG. 4

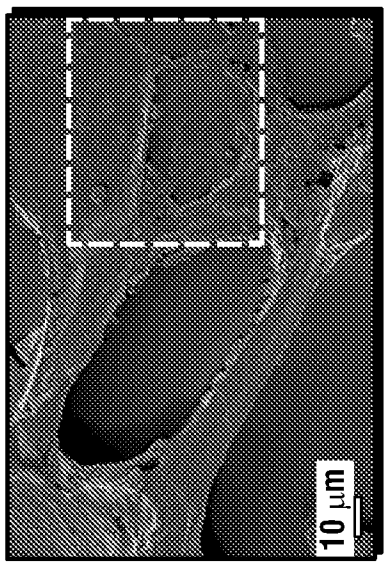

FIG. 5A

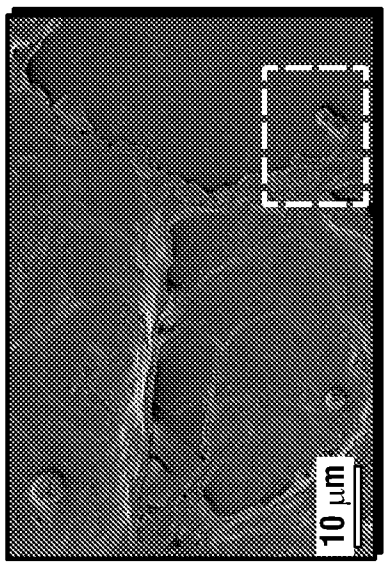

FIG. 5B

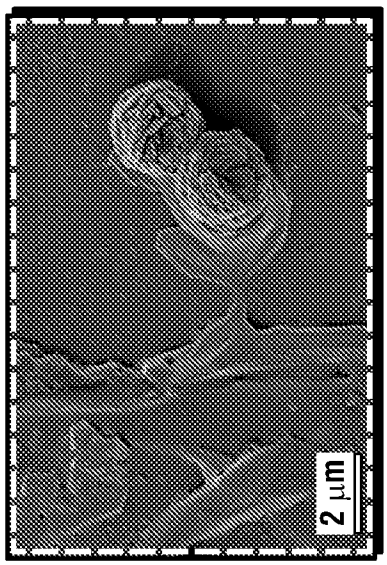

FIG. 5C

RNA oligos	1	2	3	4	5	6	7
BHQ2-5'-miR-205 sense-3'-Cholesterol	+			+	+		+
5'-miR-205 antisense-3'-Quasar705		+		+		+	+
5'-miR-221 antagomiR-3'-Quasar570			+		+	+	+

FIG. 6A

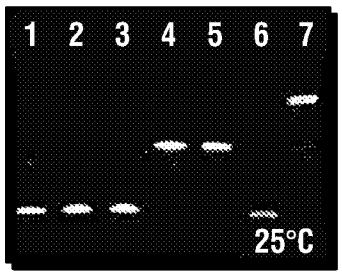

FIG. 6B

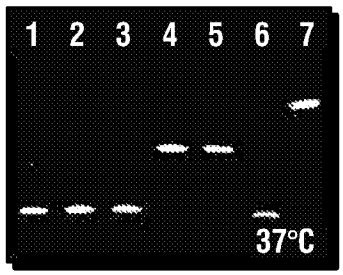

FIG. 6C

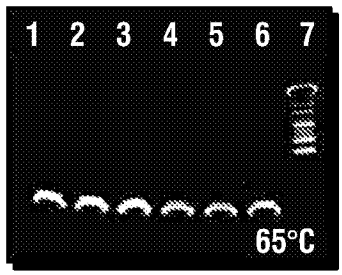

FIG. 6D

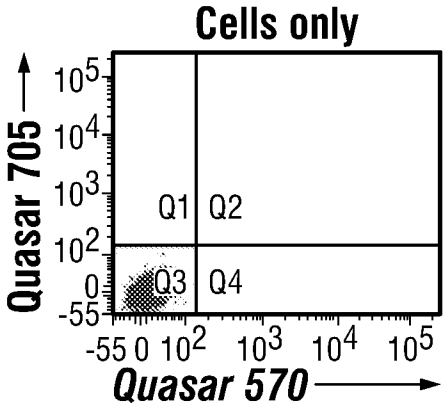

FIG. 7A

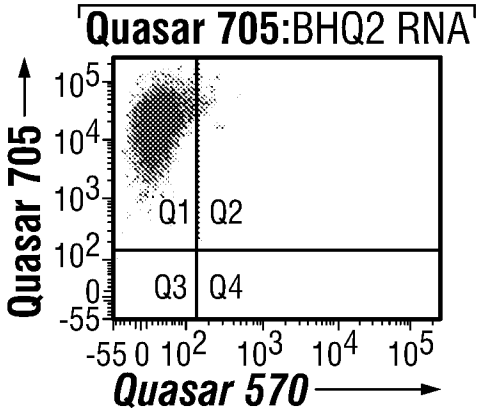

FIG. 7B

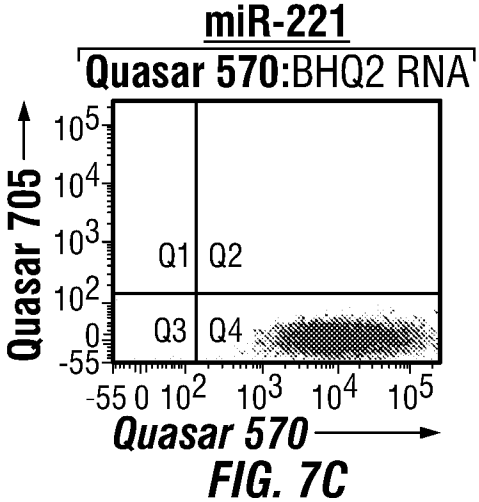

FIG. 7C

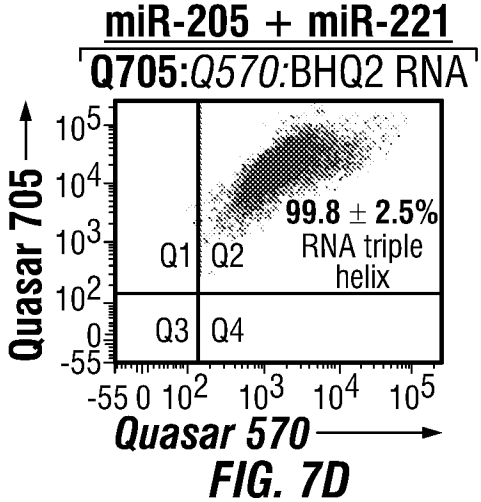

FIG. 7D

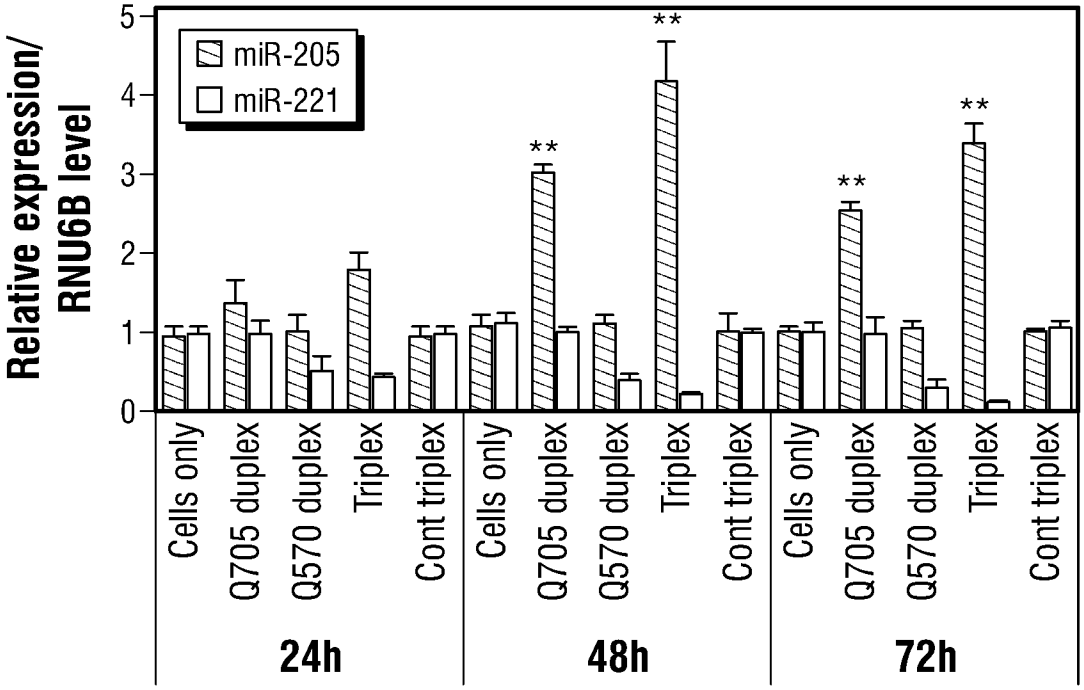
Relative expression/
RNU6B level
miR-205
miR-221
Cells only
Q705 duplex
Q570 duplex
Triplex
Cont triplex
24h
48h
72h

FIG. 8

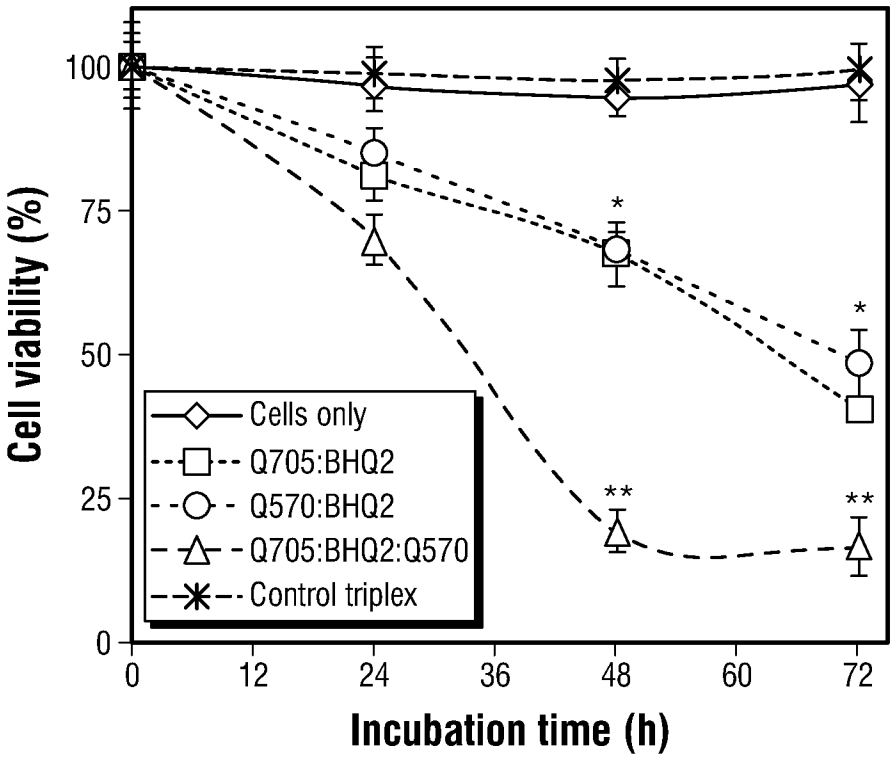
Cell viability (%)
Incubation time (h)
Cells only
Q705:BHQ2
Q570:BHQ2
Q705:BHQ2:Q570
Control triplex

FIG. 9

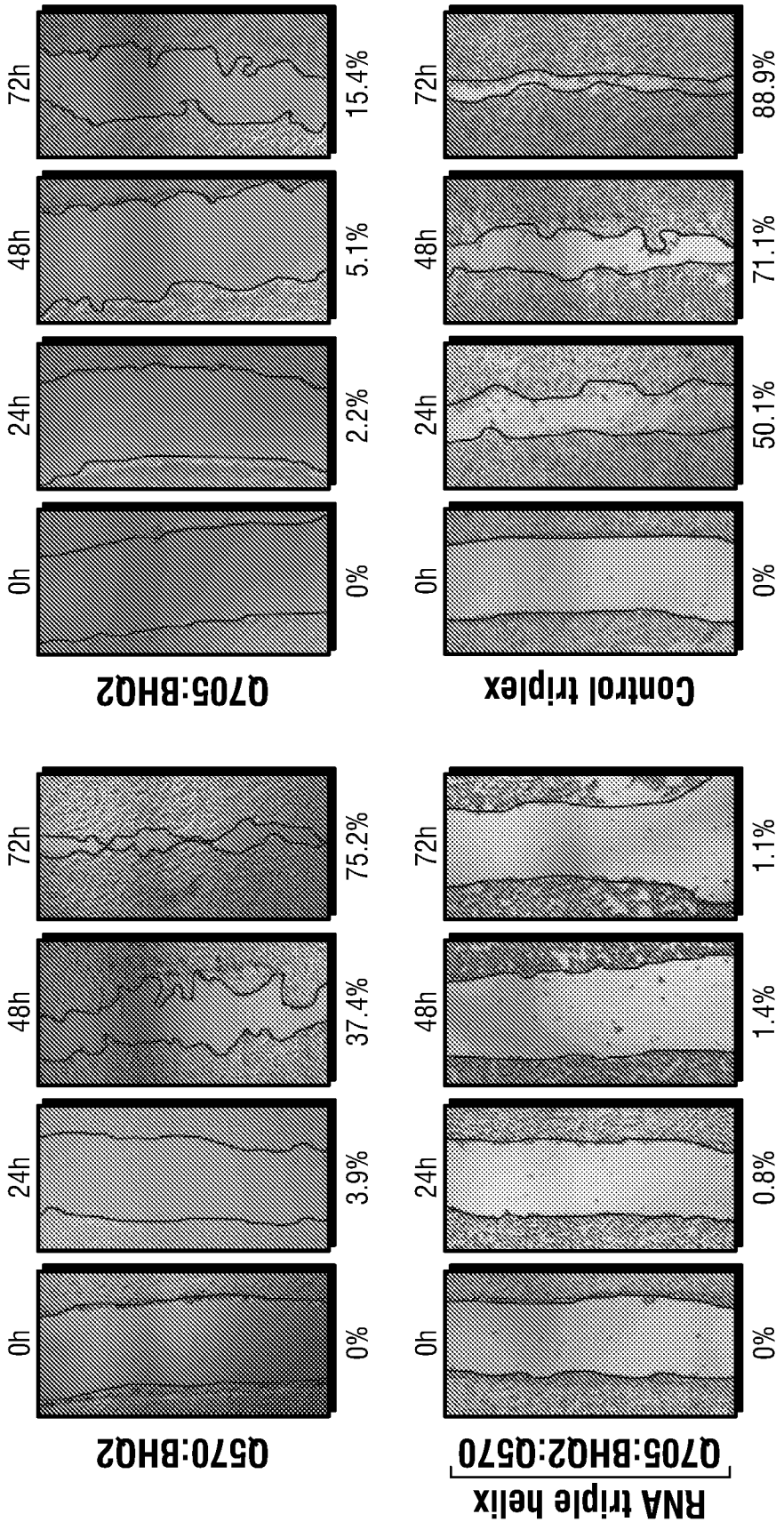
RNA triple helix
Q705:BHQ2:Q570
Q570:BHQ2
Q705:BHQ2
Control triplex
0h
24h
48h
72h
0%
3.9%
37.4%
75.2%
0.8%
1.4%
1.1%
2.2%
5.1%
15.4%
50.1%
71.1%
88.9%

FIG. 10

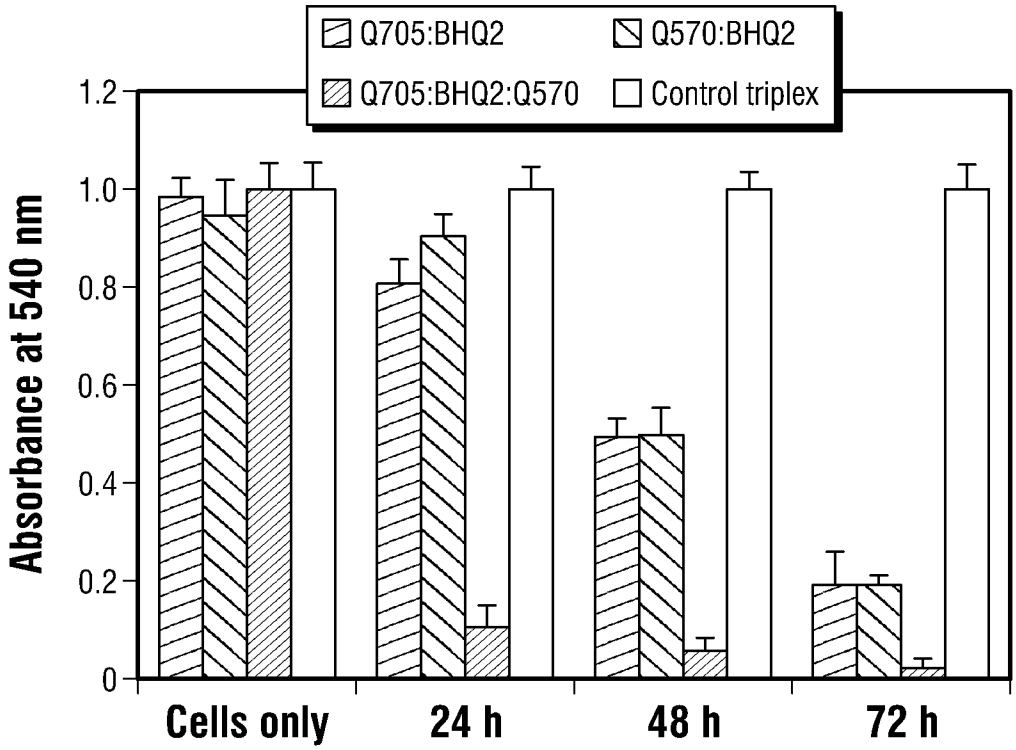
Q705:BHQ2
Q570:BHQ2
Q705:BHQ2:Q570
Control triplex
Absorbance at 540 nm
1.2
1.0
0.8
0.6
0.4
0.2
0
Cells only
24 h
48 h
72 h

FIG. 11

INTERNATIONAL SEARCH REPORT

International application No
PCT/US2016/050977

A. CLASSIFICATION OF SUBJECT MATTER
INV. C12N15/113
ADD.

According to International Patent Classification (IPC) or to both national classification and IPC

B. FIELDS SEARCHED

Minimum documentation searched (classification system followed by classification symbols)
C12N

Documentation searched other than minimum documentation to the extent that such documents are included in the fields searched

Electronic data base consulted during the international search (name of data base and, where practicable, search terms used)
EPO-Internal

C. DOCUMENTS CONSIDERED TO BE RELEVANT

Category*	Citation of document, with indication, where appropriate, of the relevant passages	Relevant to claim No.
A	WO 01/87348 A2 (UNIV MICHIGAN [US]; BAKER JAMES R JR [US]; TOMALIA DONALD A [US]) 22 November 2001 (2001-11-22) the whole document	8,34
A	WO 2011/022316 A1 (UNIV COLORADO REGENTS [US]; RICHER JENNIFER [US]; COCHRANE DAWN [US];) 24 February 2011 (2011-02-24) the whole document	4,18,27, 37
A	WO 2011/127625 A1 (JIANGSU MINGMA BIOTECH CO LTD [CN]; ZENG KE [CN]; ZHANG CHENYU [CN]; Z) 20 October 2011 (2011-10-20) the whole document	3,17,26, 36

-/--

[X] Further documents are listed in the continuation of Box C.

[X] See patent family annex.

* Special categories of cited documents :

"A" document defining the general state of the art which is not considered to be of particular relevance

"E" earlier application or patent but published on or after the international filing date

"L" document which may throw doubts on priority claim(s) or which is cited to establish the publication date of another citation or other special reason (as specified)

"O" document referring to an oral disclosure, use, exhibition or other means

"P" document published prior to the international filing date but later than the priority date claimed

"T" later document published after the international filing date or priority date and not in conflict with the application but cited to understand the principle or theory underlying the invention

"X" document of particular relevance; the claimed invention cannot be considered novel or cannot be considered to involve an inventive step when the document is taken alone

"Y" document of particular relevance; the claimed invention cannot be considered to involve an inventive step when the document is combined with one or more other such documents, such combination being obvious to a person skilled in the art

"&" document member of the same patent family

Date of the actual completion of the international search	Date of mailing of the international search report
20 December 2016	03/01/2017

Name and mailing address of the ISA/	Authorized officer
European Patent Office, P.B. 5818 Patentlaan 2 NL - 2280 HV Rijswijk Tel. (+31-70) 340-2040, Fax: (+31-70) 340-3016	Smalt, Rolf

1

Form PCT/ISA/210 (second sheet) (April 2005)

INTERNATIONAL SEARCH REPORT

International application No
PCT/US2016/050977

C(Continuation). DOCUMENTS CONSIDERED TO BE RELEVANT

Category*	Citation of document, with indication, where appropriate, of the relevant passages	Relevant to claim No.
X,P	JOÃO CONDE ET AL: "Self-assembled RNA-triple-helix hydrogel scaffold for microRNA modulation in the tumour microenvironment", NATURE MATERIALS, vol. 15, no. 3, 7 December 2015 (2015-12-07), pages 353-363, XP55330444, GB ISSN: 1476-1122, DOI: 10.1038/nmat4497 the whole document -----	1-40

1

Form PCT/ISA/210 (continuation of second sheet) (April 2005)

INTERNATIONAL SEARCH REPORT

Information on patent family members

International application No
PCT/US2016/050977

Patent document cited in search report	Publication date	Patent family member(s)	Publication date
WO 0187348 A2	22-11-2001	AU 6142001 A	26-11-2001
		BR 0110748 A	31-08-2004
		CA 2408535 A1	22-11-2001
		CN 1471407 A	28-01-2004
		CN 101347623 A	21-01-2009
		EP 1301211 A2	16-04-2003
		JP 2004515457 A	27-05-2004
		MX PA02011142 A	22-06-2004
		US 6471968 B1	29-10-2002
		US 2002165179 A1	07-11-2002
		WO 0187348 A2	22-11-2001
WO 2011022316 A1	24-02-2011	US 2012214864 A1	23-08-2012
		WO 2011022316 A1	24-02-2011
WO 2011127625 A1	20-10-2011	EP 2559442 A1	20-02-2013
		US 2013078225 A1	28-03-2013
		WO 2011127625 A1	20-10-2011